

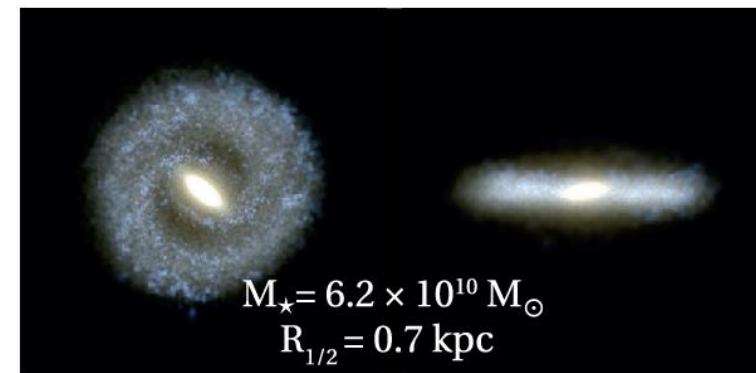
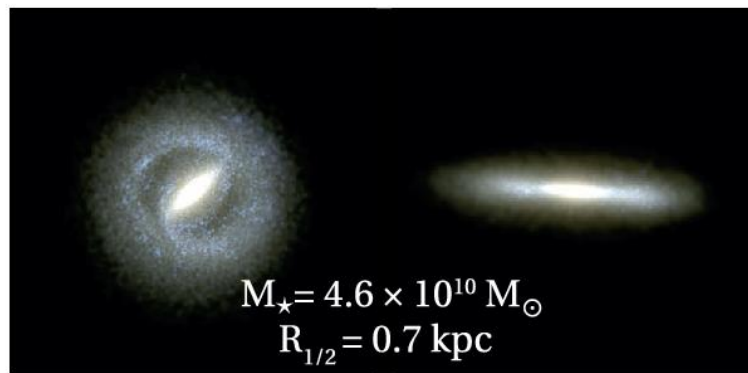
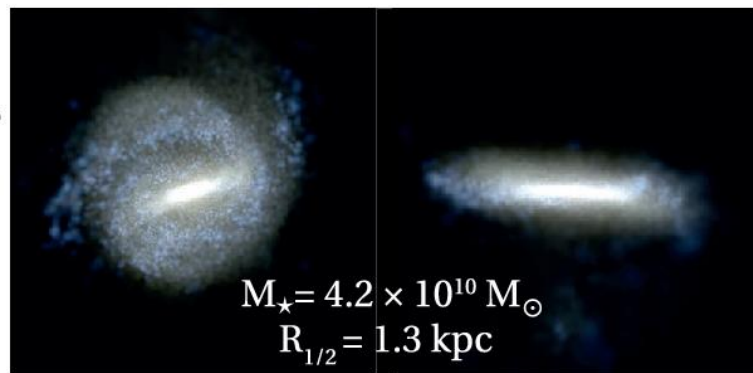


Evolution of the cosmic star-formation rate

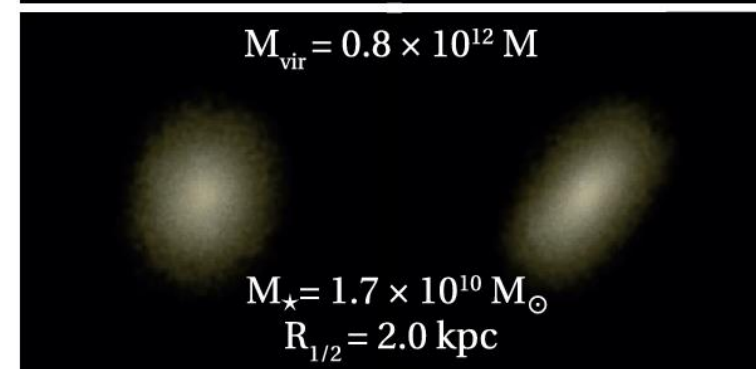
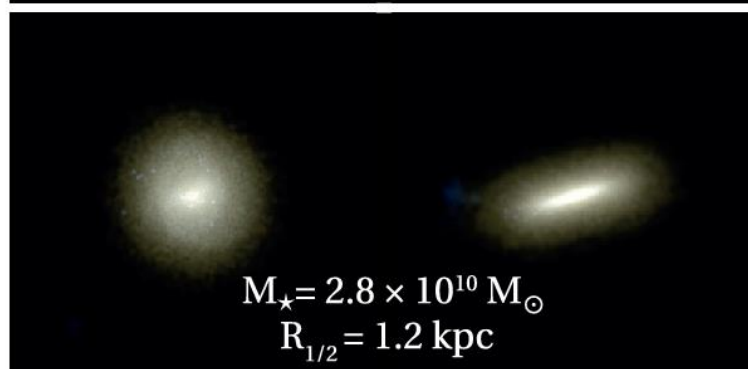
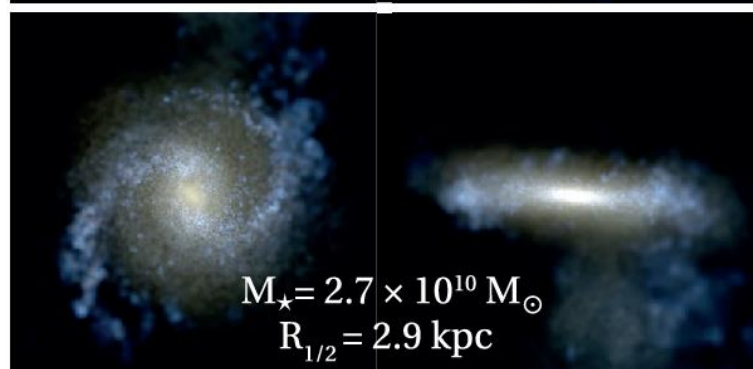
Gianfranco De Zotti

INAF – Osservatorio Astronomico di Padova

SNe only



BH+SNe



Face-on Edge-on
Suppressed merger

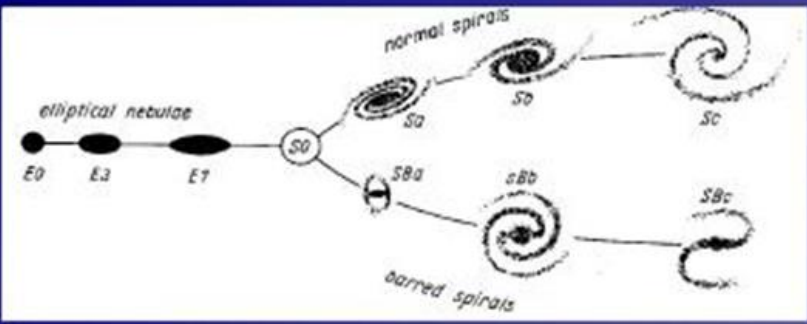
Face-on Edge-on
Reference

Face-on Edge-on
Enhanced merger

15 kpc
 15 kpc

Galaxies at $z=2.3$

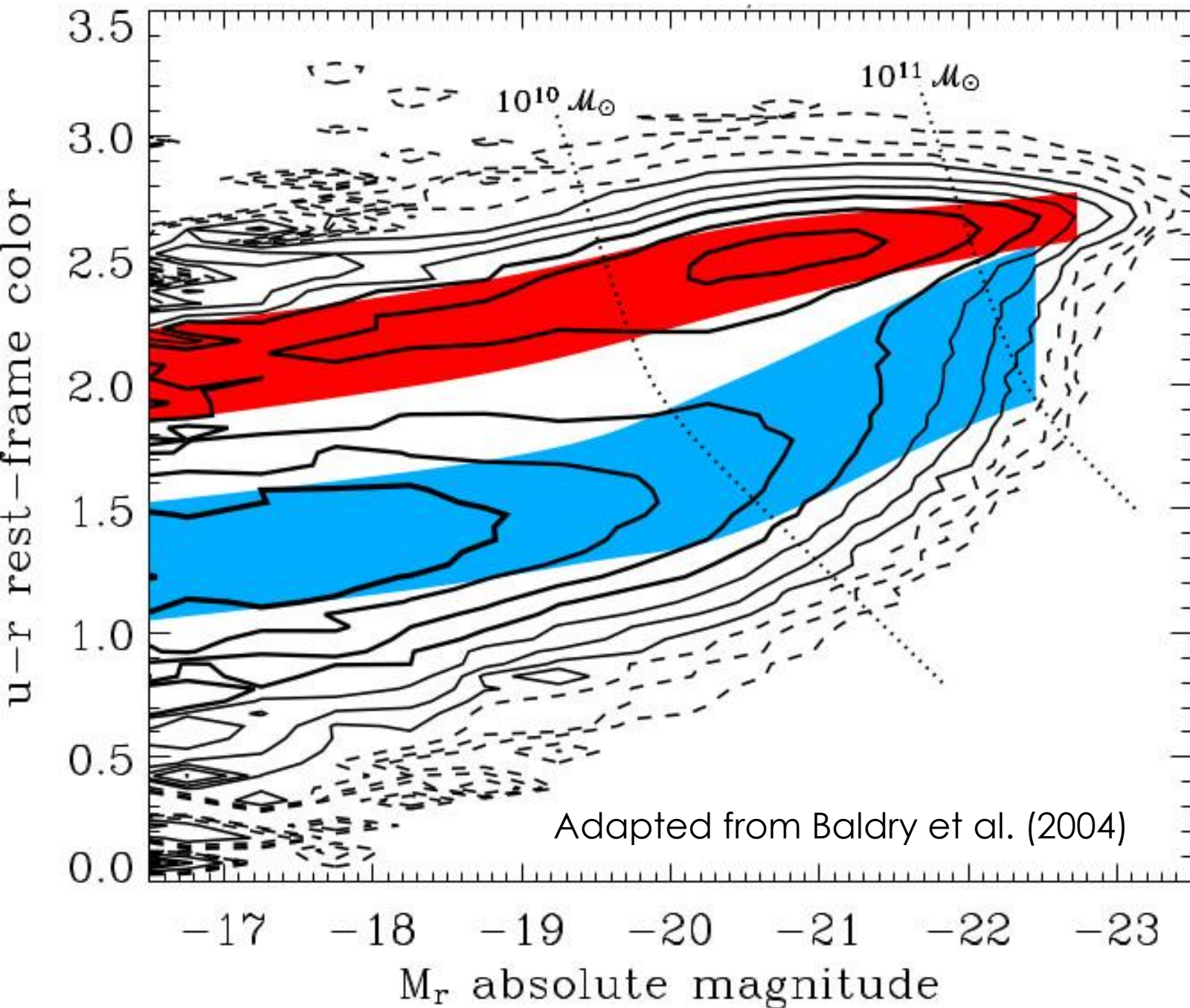
Simulated galaxies starting by zooming a cosmological simulation of a galaxy of virial mass $M_{\text{vir}} \approx 10^{12} M_{\odot}$ (Pontzen et al. 2017)



HUBBLE TUNING-FORK DIAGRAM

Following Hubble (1936), we still classify galaxies as ellipticals, spirals, and irregulars (see Sandage 2005), based on morphology. But morphology correlates with the stellar population content of these galaxies, with typical ellipticals being redder than the others and showing purely stellar absorption-line spectra with no or very weak nebular emissions.

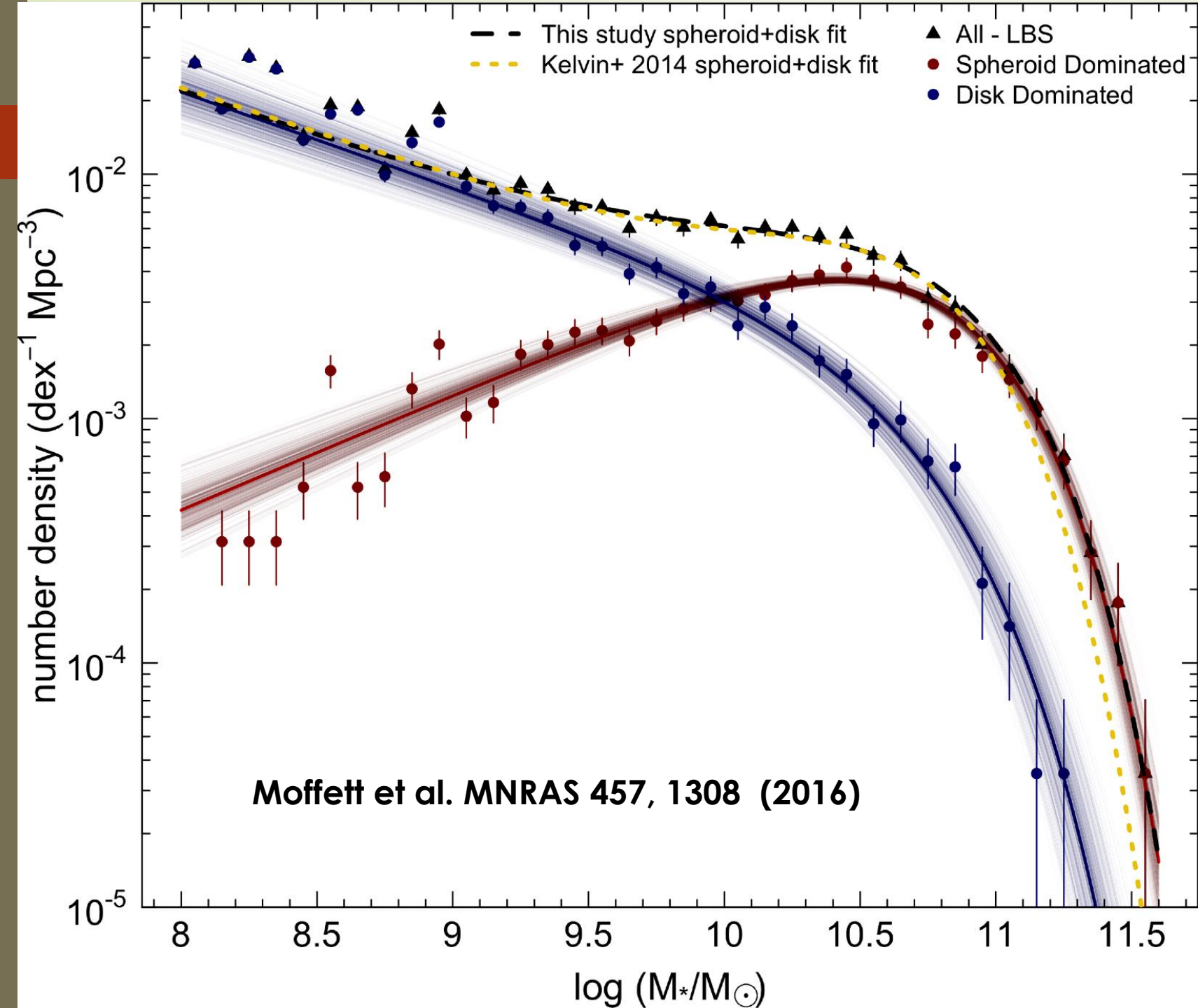




The galaxy colours bimodality reflects the bimodality of SFRs. ETGs are red, spirals are blue. Only a small fraction of galaxies have intermediate colours (Green Valley galaxies). This suggests that star formation in galaxies is either ongoing or was quenched several Gyr ago. Green Valley galaxies should have experienced a recent quenching of their star formation. Seyfert galaxies have intermediate age stellar populations (Schawinski et al. 2007) and mostly lie in the Green Valley (Schawinski 2012). This suggests that star formation is quenched by nuclear activity.

Spheroid- vs disk-dominated galaxies

- A consequence of the morphology-colour correlation is that one often refers to early-type galaxies (ETG), even if they are colour (or spectral-type) selected rather than morphologically selected.
- The bulges of spirals of the earlier types show morphological as well as spectral similarities with ellipticals, and one often includes both ellipticals and bulges under the category of galactic spheroids.
- The correlation between colour and morphology selection persists up to substantial redshift, e.g., at $z \sim 0.7$ about 85% of color-selected, red-sequence galaxies are also morphologically early-type, i.e., E/S0/Sa (Bell et al. 2004), an estimate broadly consistent with the local one, when allowing for the broader morphological criterion.
- The space density of spheroids (excluding little blue spheroids, LBS) is lower than that of disks, but their mean stellar mass is much higher. As a result, spheroids contain the majority of the stellar mass.



Comparison of the stellar mass functions of disk- and spheroid-dominated galaxies (without the little blue spheroids, LBS). Spheroids dominate the galaxy stellar mass function above $\sim 10^{10} M_{\text{sun}}$. Approximately 70% of the total stellar mass is found in spheroid-dominated systems (E and S0-Sa) and approximately 30% per cent in disc-dominated systems (Sab-Scd and Sd-Irr). However, this depends on how we deal with bulges.



Only less than 10% of baryons make stars!

Galaxy formation
is
shokingly inefficient

More than 90% of baryons are elsewhere!

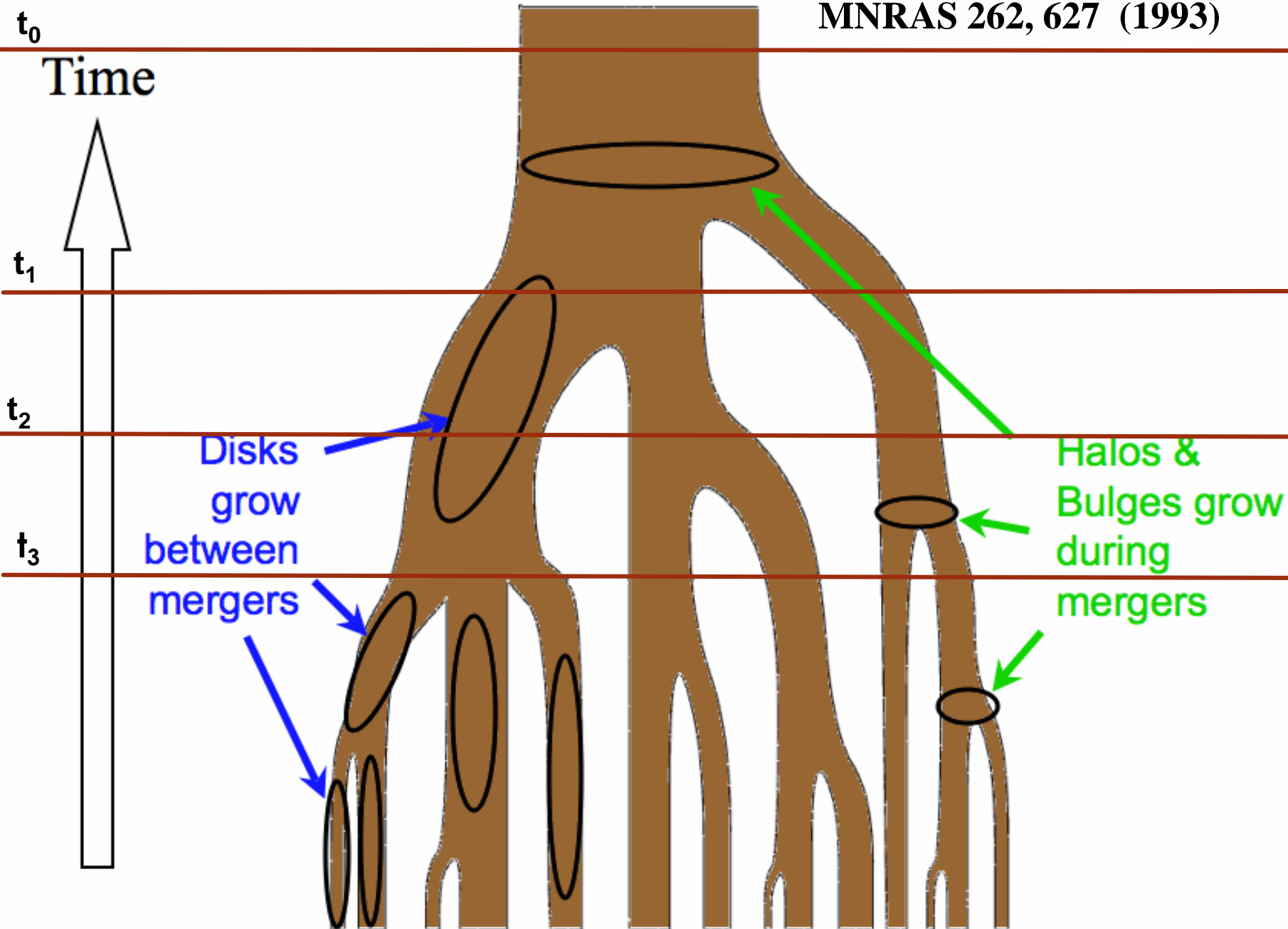
Parameter	In red Planck results (Planck Collaboration XIII 2016)	Components ^a	Totals ^a	Total visible matter: $\Omega_{\text{vis}} =$ 0.00525, i.e. ~ 10.5% of baryons; total baryons in galaxies: $\Omega_{\text{gal}} =$ 0.00345, i.e. ~ 8% of baryons.
Dark sector:			0.954 ± 0.003	
Dark energy		0.72 ± 0.03	0.951 ± 0.023	
Dark matter		0.23 ± 0.03	0.6911 ± 0.0062	
Primeval gravitational waves		$\lesssim 10^{-10}$	0.2589 ± 0.0022	
Primeval thermal remnants:			0.0010 ± 0.0005	
Electromagnetic radiation		$10^{-4.3 \pm 0.0}$		
Neutrinos		$10^{-2.9 \pm 0.1}$		
Prestellar nuclear binding energy		$-10^{-4.1 \pm 0.0}$		
Baryon rest mass:			0.045 ± 0.003	
Warm intergalactic plasma			0.040 ± 0.003	
Virialized regions of galaxies	0.024 ± 0.005			
Intergalactic	0.016 ± 0.005			
Intracluster plasma		0.0018 ± 0.0007		
Main-sequence stars: spheroids and bulges		0.0015 ± 0.0004		
Main-sequence stars: disks and irregulars		0.00055 ± 0.00014		
White dwarfs		0.00036 ± 0.00008		
Neutron stars		0.00005 ± 0.00002		
Black holes		0.00007 ± 0.00002		
Substellar objects		0.00014 ± 0.00007		
H I + He I		0.00062 ± 0.00010		
Molecular gas		0.00016 ± 0.00006		$\epsilon_n \approx 0.1$: radiation efficiency
Planets		10^{-6}		
Condensed matter	Fukugita & Peebles (2004)	$10^{-5.6 \pm 0.3}$		
Sequestered in massive black holes		$10^{-5.4}(1 + \epsilon_n)$		

Galaxy vs halo mass function

- 
- 
- ▶ Why is the shape of the galaxy stellar mass function different from the halo mass function?
 - ▶ Why is there an upper limit to the galaxy stellar mass function?

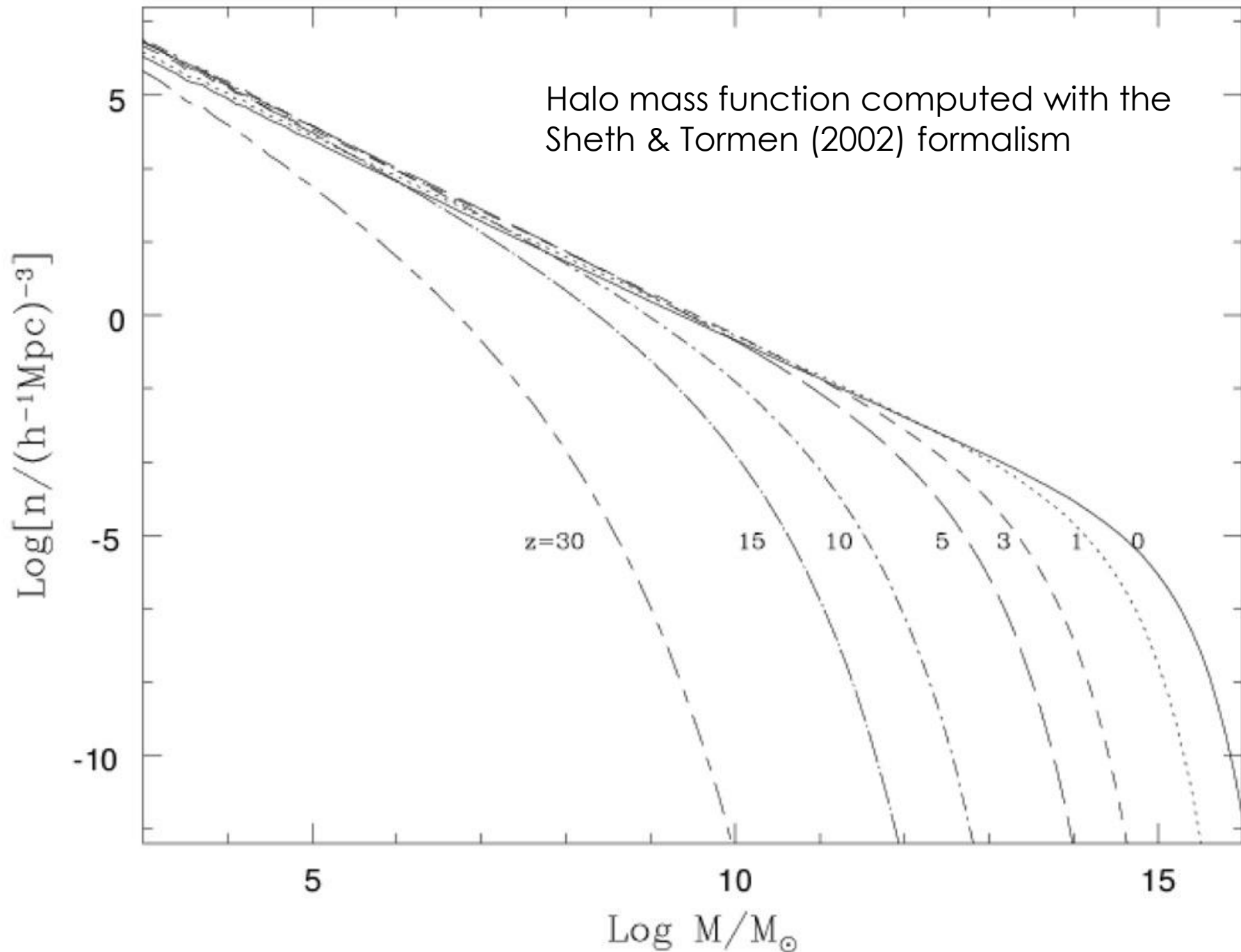
Merger Tree

Adapted from Lacey & Cole
MNRAS 262, 627 (1993)



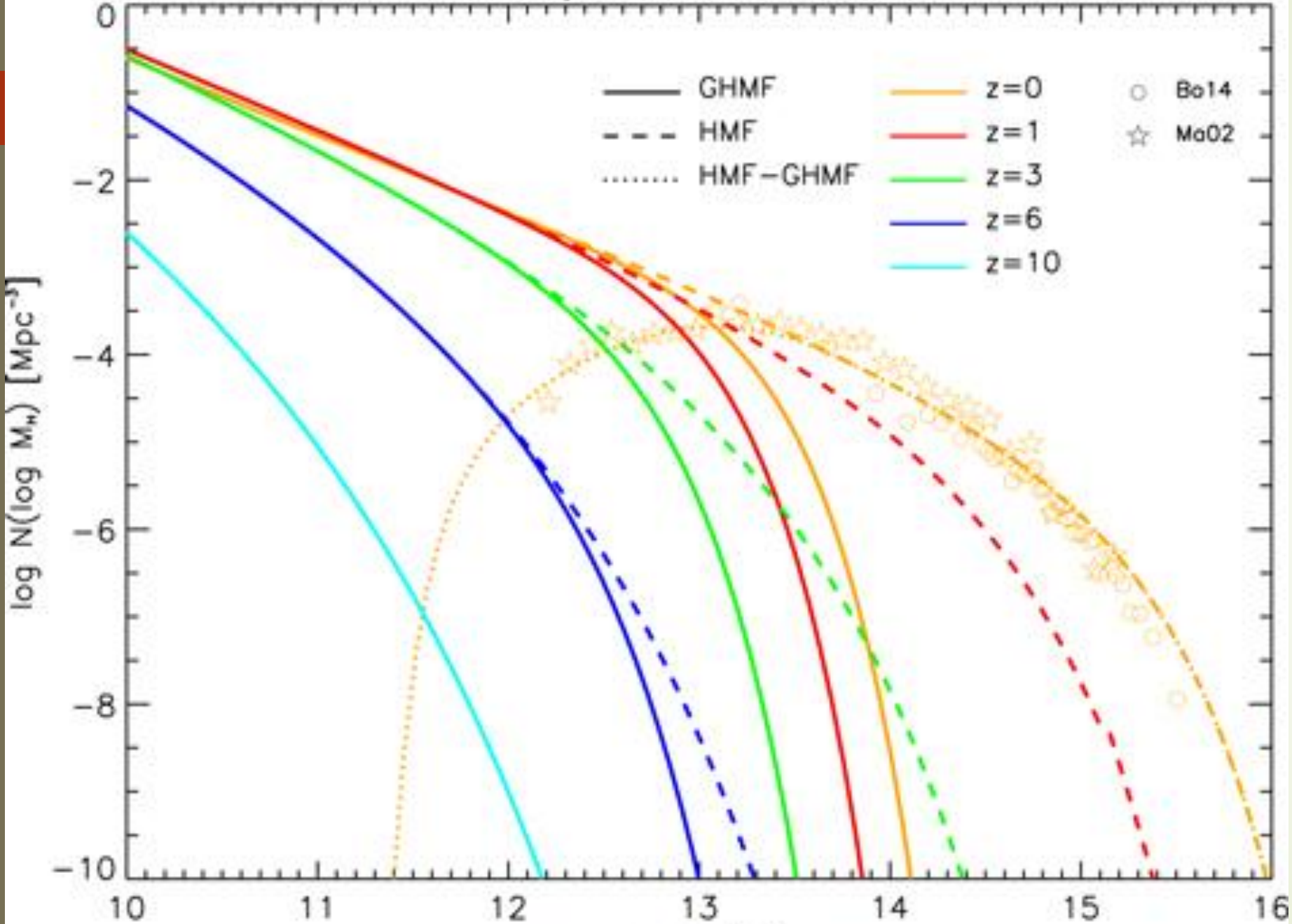
Galaxy vs halo mass function -1

Schematic representation of a 'merger tree' depicting the growth of a halo as the result of a series of mergers. The widths of the branches represent the masses of the individual parent haloes. A slice through the tree horizontally gives the distribution of masses in the parent haloes at a given time. t_0 is the present time and t_3 is the formation time, defined as the time at which a parent halo containing in excess of half of the mass of the final halo was first created.



The halo mass function evolves strongly with redshift. At the present time it smoothly extends to masses $> 10^{15} M_{\text{sun}}$. But this is not the case for the stellar mass function.

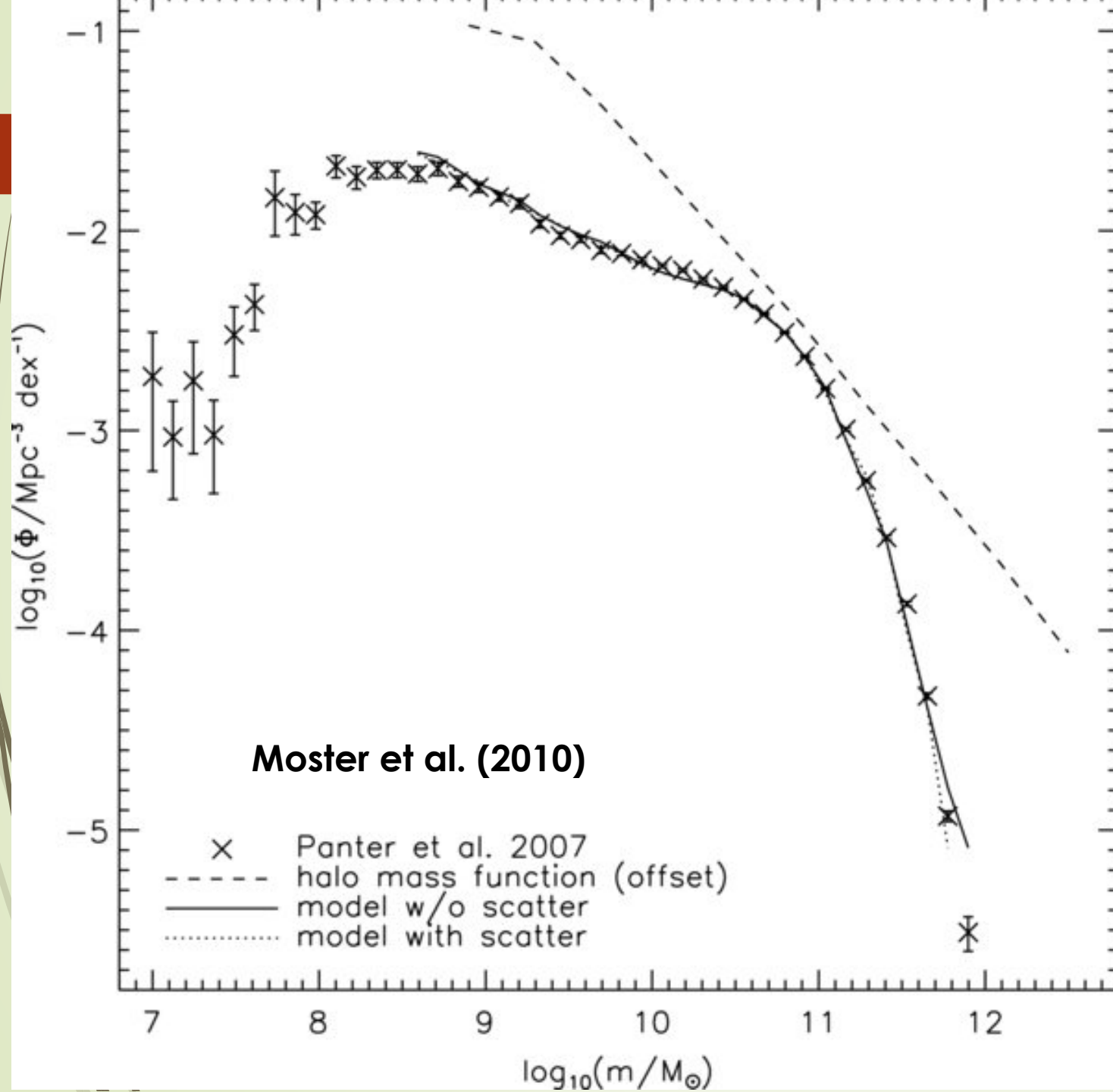
Galaxy Halo Mass Function



Comparison of the galaxy halo mass function (GHMF, solid lines) with the total halo mass function (HMF, dashed) at different z . The GHMF is obtained from the HMF by adding the global sub-halo mass function and subtracting the mass function of multiply-occupied halos. The dotted line at $z = 0$ shows the cluster and group halo mass function, obtained by subtraction of the solid from the dashed line. This is compared with the determinations by Boehringer et al. (2014; circles) and by Martinez et al. (2002; stars).

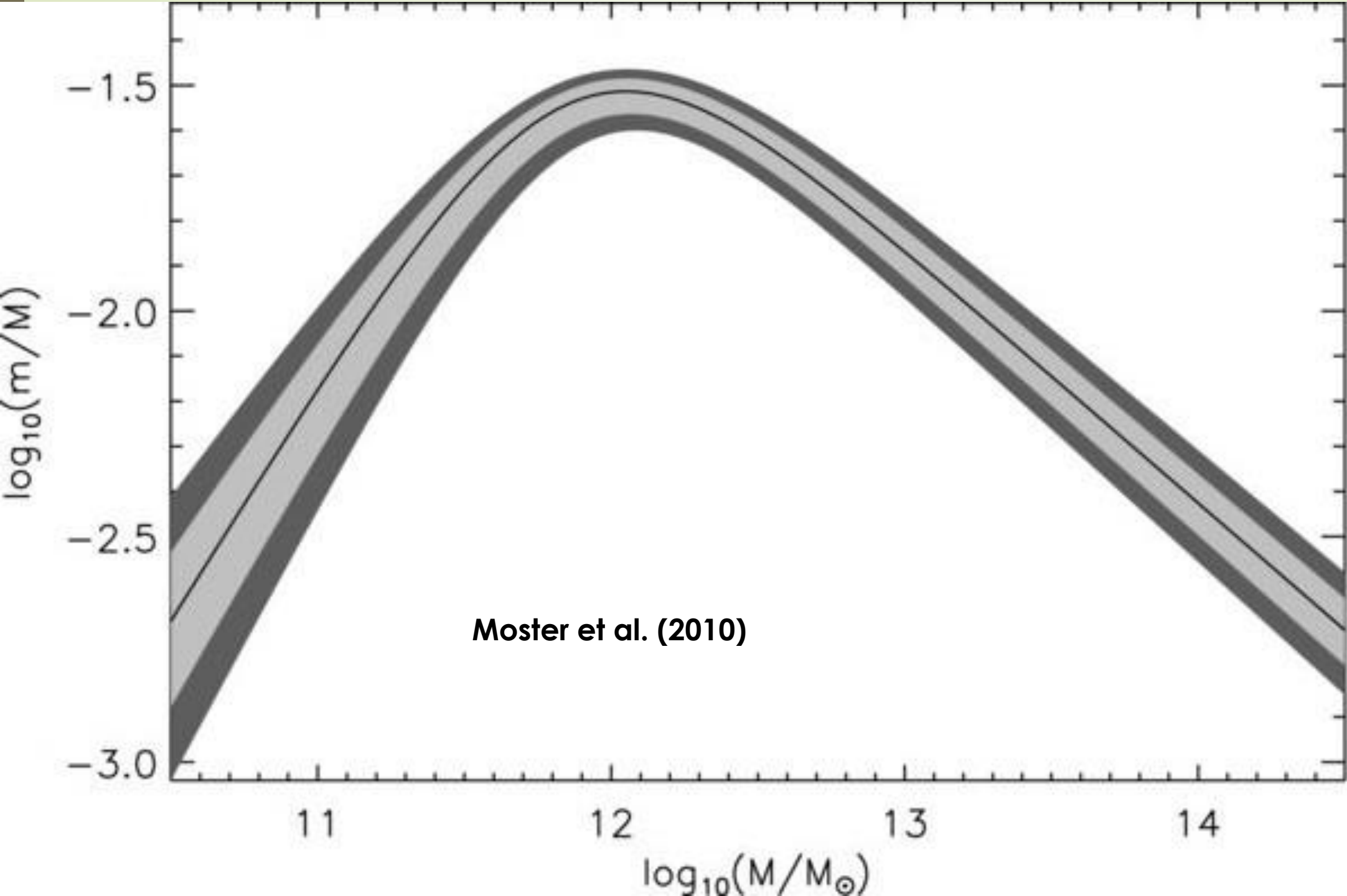
Aversa et al. (2015)

$\log M_h [M_\odot]$



Comparison between the halo mass function **offset by a factor of 0.05** (dashed line), the observed local galaxy stellar mass function (Panter et al. 2007; symbols) and model by Moster et al. (2010) with (dotted line) and without scatter (solid line). The drop at low mass of the observed stellar mass function is due to incompleteness.

The halo and the galaxy mass functions have different shapes, implying that the stellar-to-halo mass ratio m/M is not constant. The closest approach is for $m \approx 3 \times 10^{10} M_{\text{sun}}$.



Moster et al. (2010)

Ratio of stellar, m , to halo mass, M , as a function of M , derived using the *abundance matching technique*. The light shaded area shows the 1σ region while the dark and light shaded areas together show the 2σ region. The maximum star formation efficiency corresponds to $M \sim 10^{12} M_{\text{sun}}$.

The comparison of the stellar to halo mass function identifies a characteristic galactic *halo* mass $M_h \sim 10^{12} M_\odot$.

M_h is understood by the requirement that cooling within a dynamical time is a necessary condition for efficient star formation.

Define $t_{\text{cool}} = 3/2nkT/[n^2\Lambda(T)]$ and $t_{\text{dyn}} = 3/(\sqrt{32\pi G\rho})$. For star formation to occur, cooling is essential, and the condition $t_{\text{cool}} < t_{\text{dyn}}$ guarantees cooling in an inhomogeneous galactic halo where gas clouds collide at the virial velocity.

One finds that (Silk 1977, Silk & Mamon 2012)

$$M_{\text{cool}}^* = \frac{\alpha^3}{\alpha_g^2} \frac{m_p}{m_e} \frac{t_{\text{cool}}}{t_{\text{dyn}}} T^{1+2\beta},$$

where $\alpha = e^2/(\hbar c)$ and $\alpha_g = Gm_p^2/e^2$ are the electromagnetic and gravitational fine structure constants.

The condition $t_{\text{cool}} = t_{\text{dyn}}$ than defines a critical halo mass $\sim 10^{12} M_\odot$ (Silk 1977), corresponding to a stellar mass of $\sim 3 \times 10^{10} M_\odot$, and to a typical $L_\star \sim \text{a few} \times 10^{10} L_\odot$ for a typical mass-to-light ratio $M/L \sim \text{a few}$.

- 
- 
- Why is the star-formation efficiency decreasing as we move away from the characteristic halo mass?
 - The current favourite answer is **feedback**
 - There are various flavours of feedback, but those thought to have the main role are supernova explosions and AGN activity.

- Supernova feedback may affect the surrounding gas by transferring kinetic energy to it and giving the gas enough velocity to escape the galaxy.
- The cold gas removal rate by supernova explosions, $\dot{M}_{\text{cold}}^{\text{SN}}$ can be written as (Granato et al. 2004; Lapi et al. 2014):

$$\dot{M}_{\text{cold}}^{\text{SN}} = \frac{N_{\text{SN}} \epsilon_{\text{SN}} E_{\text{SN}}}{\epsilon_{\text{bind}}} \text{SFR} ,$$

where $N_{\text{SN}} \approx 1.4 \times 10^{-2} / M_{\odot}$ is the number of SNe per unit solar mass condensed into stars, $E_{\text{SN}} \approx 10^{51}$ erg is the kinetic energy released per SN explosion,

$\epsilon_{\text{bind}} \approx 3 \times 10^{14} (M_{\text{H}} / 10^{12} M_{\odot})^{2/3} [(1+z)/3.5] \text{ cm}^2 \text{ s}^{-2}$ is the *specific* binding energy of the gas in the halo; $\epsilon_{\text{SN}} \sim 0.05$ is the standard value adopted for the SN feedback efficiency (e.g., White & Frenk 1991; Cole et al. 2000).

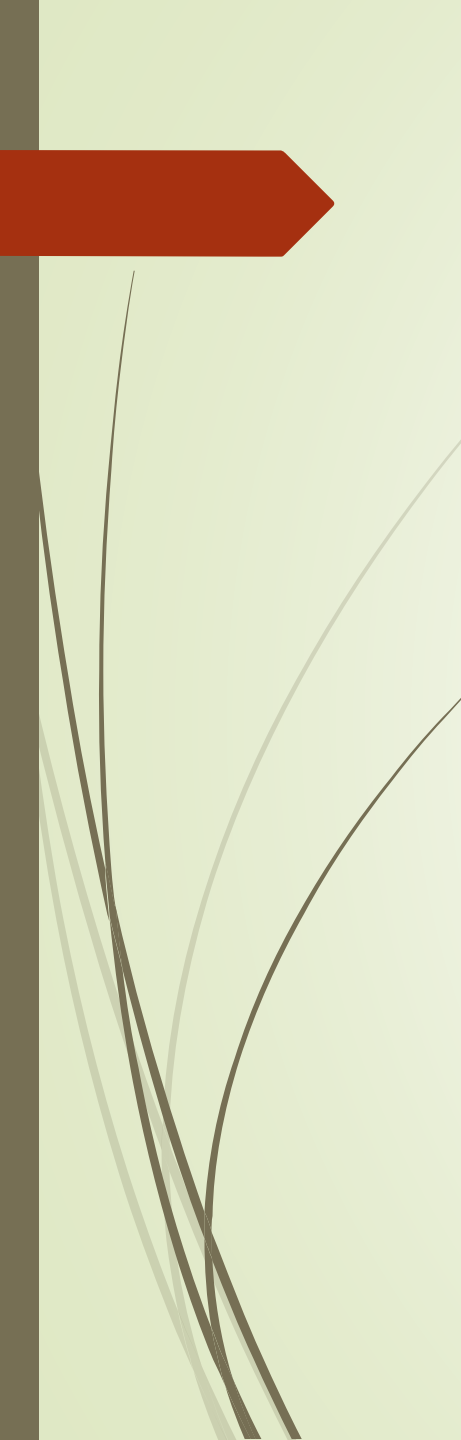
The gas binding energy is then

$$E_{\text{bind}} = M_{\text{gas}} \epsilon_{\text{bind}} \approx 6 \times 10^{57} \frac{M_{\text{gas}}/M_{\text{H}}}{0.01} \left(\frac{M_{\text{H}}}{10^{12} M_{\odot}} \right)^{5/3} \frac{1+z}{3.5} \text{ erg.}$$

Thus, at $x \simeq 2.5$ and for $M_{\text{gas}} \sim 0.01 M_{\text{H}}$ the kinetic energy of a single SN exceeds the gas binding energy for $M_{\text{H}} \lesssim 10^8 M_{\odot}$.

Taking into account the SN feedback efficiency ($\epsilon_{\text{SN}} \sim 0.05$), a single SN can expel all the cold gas from a galaxy with $M_{\text{H}} \lesssim 4 \times 10^6 M_{\odot}$.

For larger galaxies, the feedback involves the combined action of many SNaE and the balance of the energy supplied by them with that dissipated in collisions between cold gas clouds.

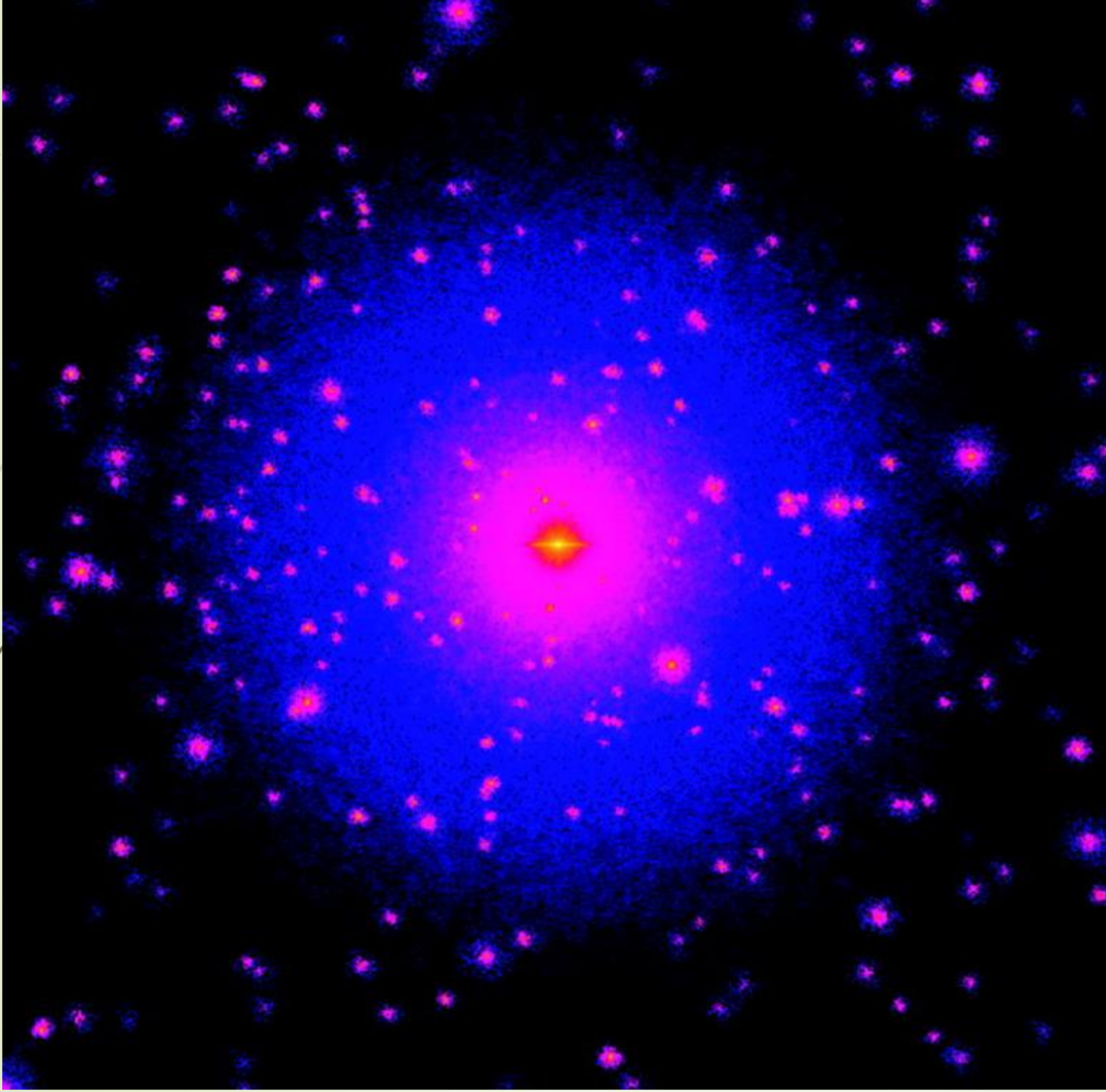


According to the simulations by Efsthathiou (2000), in a Milky Way-type system (i.e. $M_H \sim 10^{12} M_\odot$) feedback from SNaE may drive out some of the gas from the halo in the early phases of evolution ($t \lesssim 0.3$ Gyr) when the star formation rate is high and the temperature of the hot phase exceeds $\sim 5 \times 10^6$ K. For plausible sets of parameters, perhaps 20 – 30% of the final stellar mass might escape from the galaxy. At later times, the temperature of the hot phase drops to $\sim 10^6$ K and the evaporated gas cycles within the halo in a galactic fountain.

The energy injected by SNaE into the ISM also regulates the star formation efficiency (SFE). SNe provide recirculation and venting of gas into fountains, thereby reducing the SFE and prolonging the duration of star formation in normal disk galaxies, that are the dominant population for $M_H \lesssim 10^{12} M_\odot$.

According to Silk & Mamon (2012), SN feedback accounts for typical SFE ~ 0.02 .

Font et al. (2001)



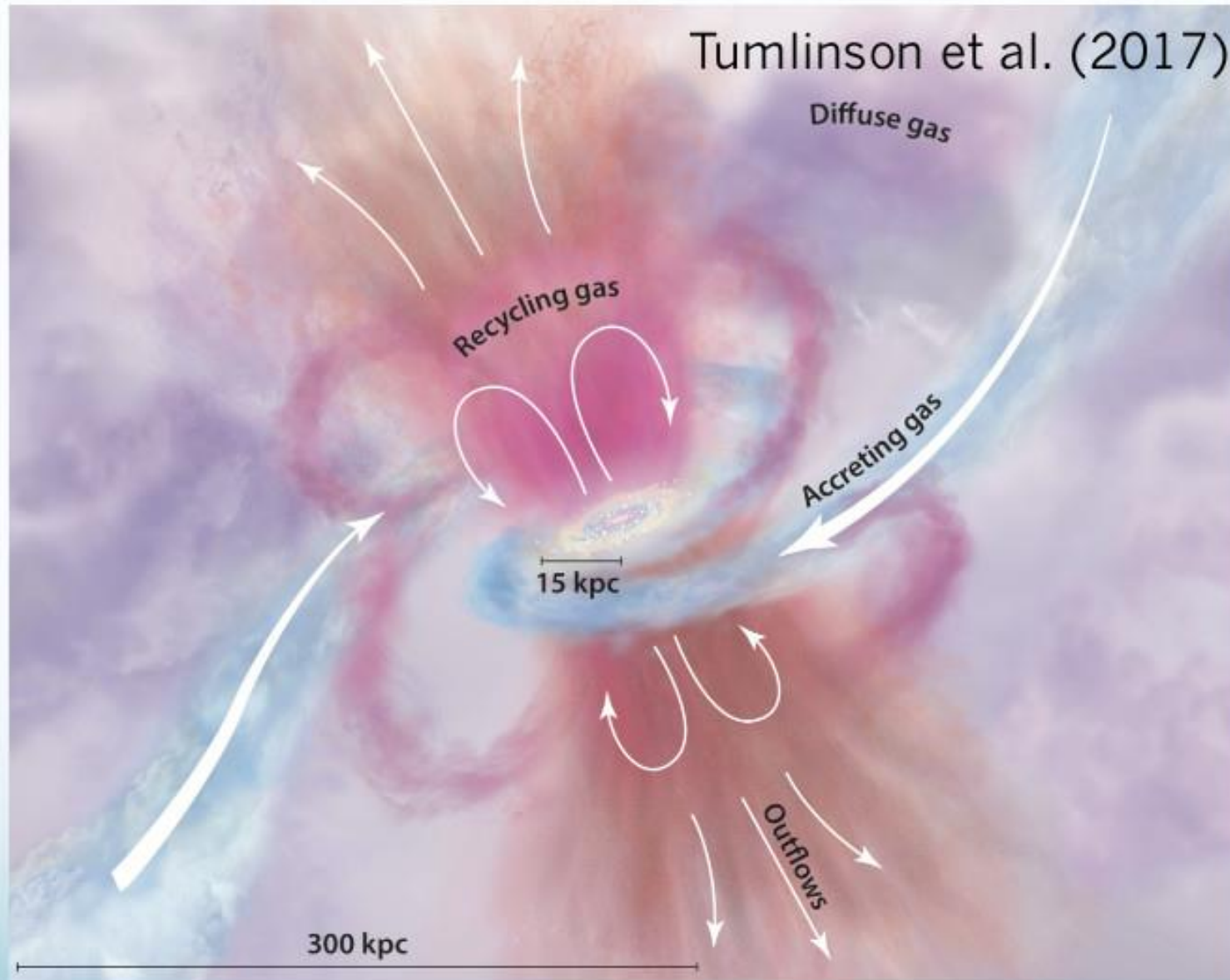
This



is really ...

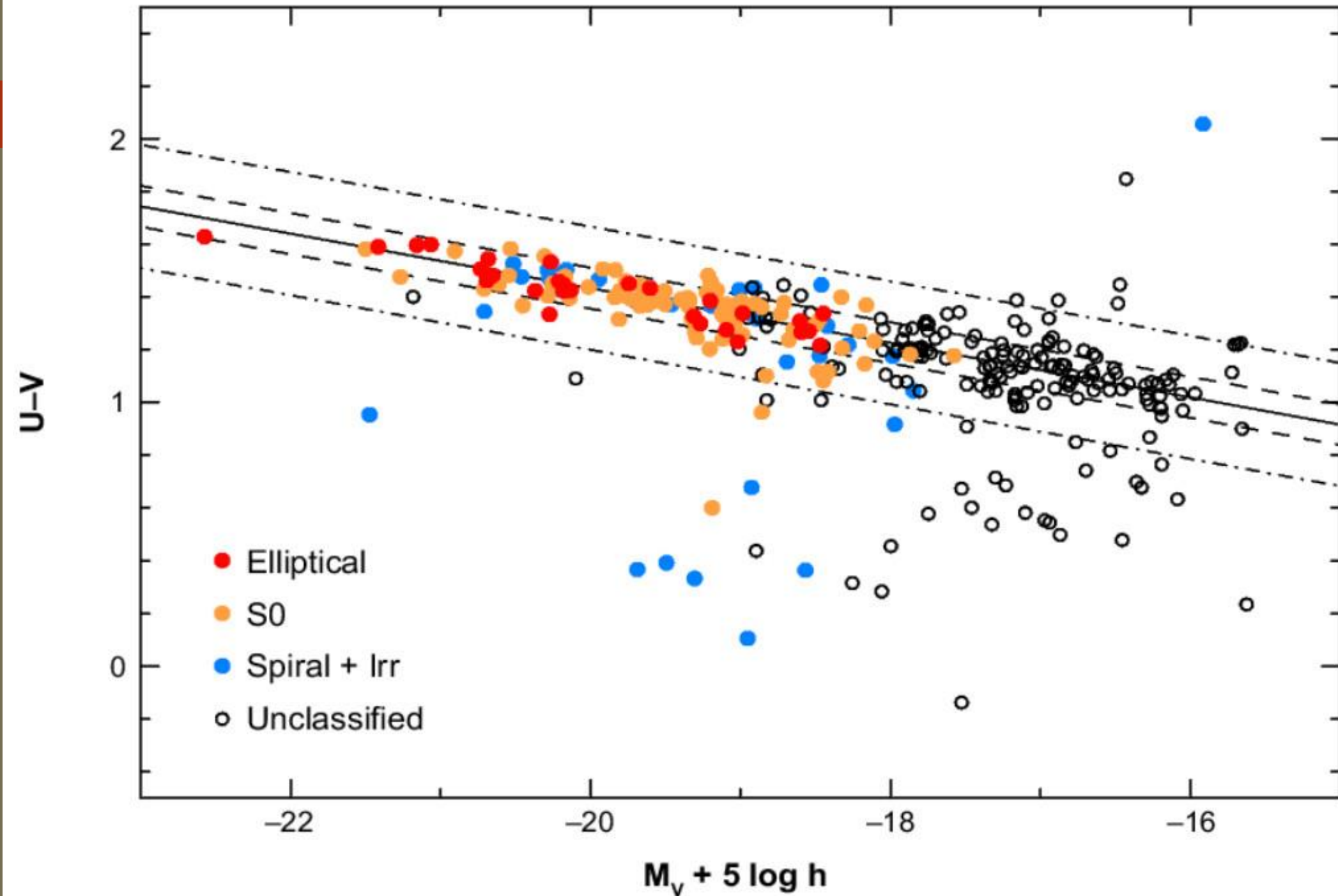
Source: J. Bartlett

That:

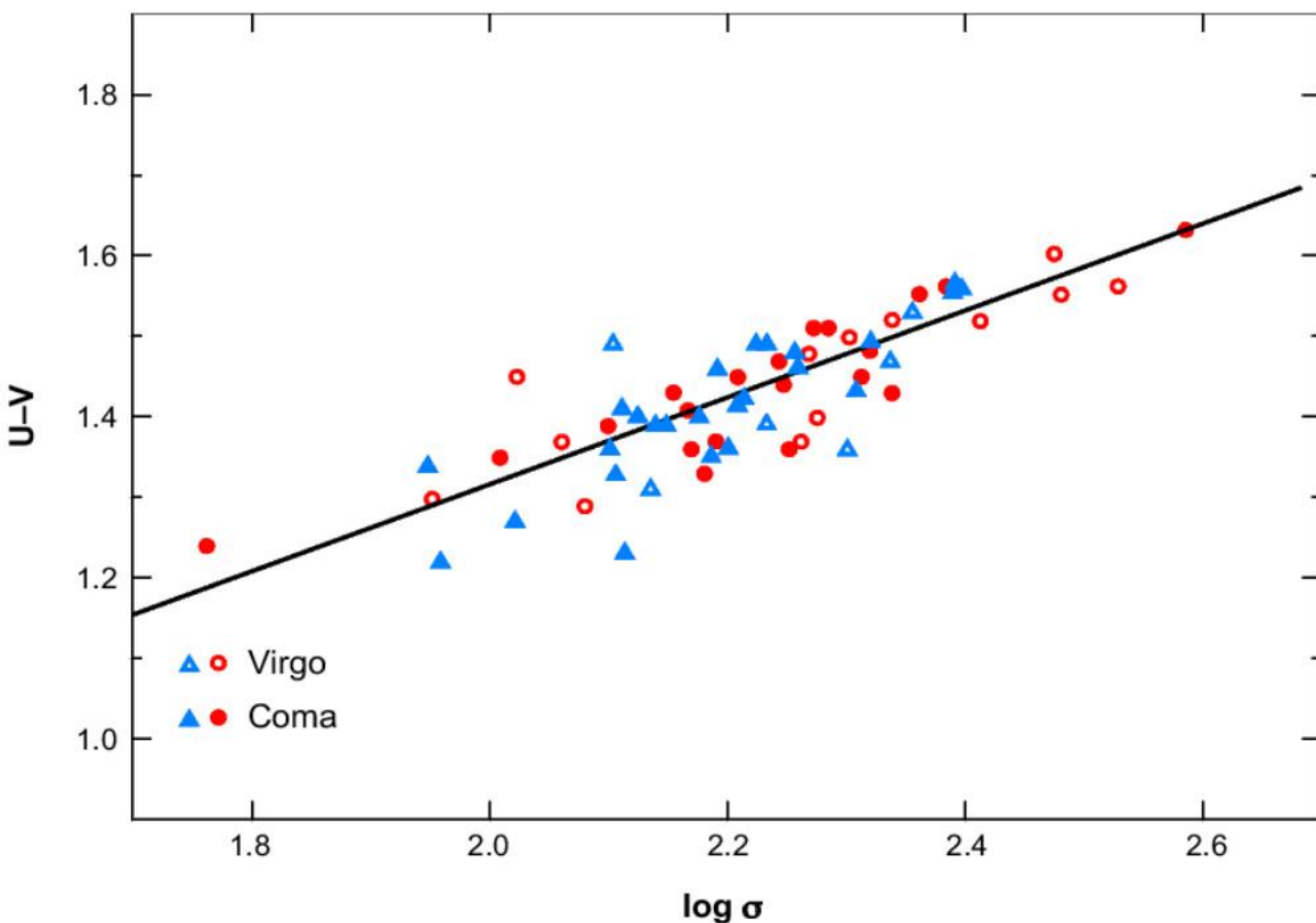


Spheroidal galaxies

- ▶ Spheroidal galaxies dominate the galaxy stellar mass function for $M_* > 10^{10} M_{\text{sun}}$.
- ▶ Again the baryon fraction is far from its primordial value, but SNaE cannot eject significant amounts of gas from massive galaxies.
- ▶ In the early simplest version of hierarchical growth of galaxies, baryons continue to be accreted over a Hubble time and the stellar mass grows. Consequences:
 - ▶ Massive galaxies are overproduced
 - ▶ Are too blue since the star formation continues down to low z
 - ▶ Form late because massive halo preferentially form late.



ETGs follow a tight color-magnitude (C-M) relation (Baum 1959; Visvanathan & Sandage 1977). Sandage & Visvanathan (1978a,b) established the universality of this relation. The $(U - V) - M_V$ color-magnitude relation for galaxies that are spectroscopic members of the Coma cluster (Bower et al. 1999).



Relation between $(U - V)$ and central velocity dispersion (σ) for ETGs in the Virgo (open symbols) and Coma (filled symbols) clusters. Red circles represent ellipticals; blue triangles represent S0s. From Bower, Lucey & Ellis (1992).

The colour-velocity dispersion relation

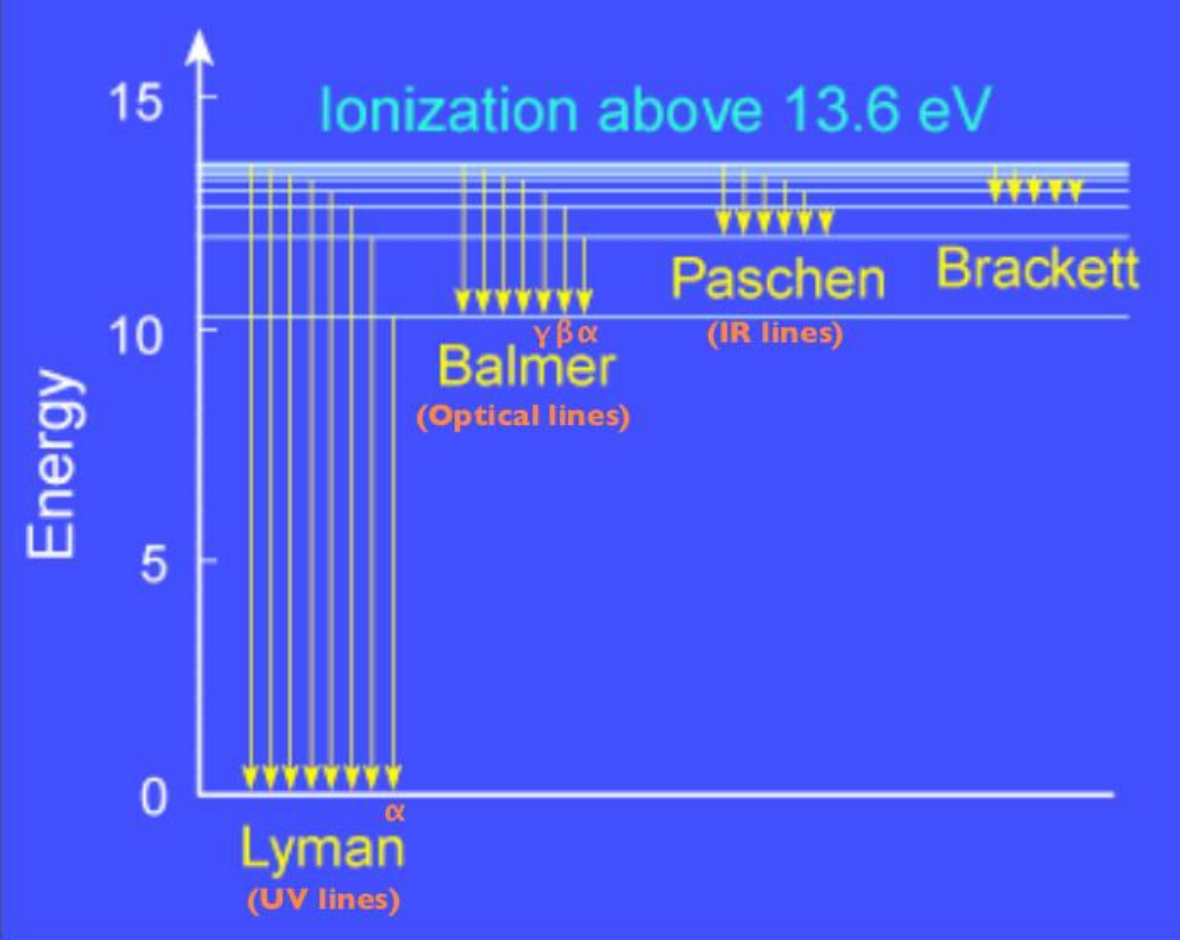
- ▶ Bower et al. (1992) reported a remarkable homogeneity of ETGs in the Virgo and Coma clusters. They estimated the intrinsic colour scatter in the colour- σ relation to be $\delta(U - V) \leq 0.04$ mag.
- ▶ They concluded that if the scatter is attributed to an age dispersion, ellipticals in clusters formed the bulk of their stars at $z \geq 2$, and later additions should not provide more than $\sim 10\%$ of their present luminosity. This approach provided, for the first time, a robust demonstration that cluster ellipticals are made of very old stars.
- ▶ The slope of the C-M and colour- σ relations sets constraints on the amount of merging that may have led to the present-day galaxies: merging without star formation increases luminosity and σ , but leaves colors unchanged, thus broadening and flattening the relations. Merging with star formation makes bluer galaxies, thus broadening and flattening the relations even more.
- ▶ Bower et al. (1998) concluded not only that the bulk of stars in clusters must have formed at high redshift, but also that they cannot have formed in mass units much less than about half their present mass.

The fundamental plane

- ▶ Three key observables of elliptical galaxies, namely the effective radius R_e , the central velocity dispersion σ , and the luminosity L , or equivalently the effective surface brightness $I_e = L/2\pi R_e^2$, relate their structural/dynamical status to their stellar content.
- ▶ Elliptical galaxies are not randomly distributed within the 3D space (R_e, σ, I_e) , but rather cluster close to a plane, thus known as the fundamental plane (FP), with $R_e \propto \sigma^a I_e^b$ (Dressler et al. 1987, Djorgovski & Davis 1987), where the exponents a and b depend on the specific band used for measuring the luminosity.
- ▶ The mere existence of a FP implies that ellipticals:
 - ▶ are well-virialized systems,
 - ▶ have self-similar (homologous) structures, or their structures (e.g., the shape of the mass distribution) vary in a systematic fashion along the plane,
 - ▶ and contain stellar populations that must fulfill tight age and metallicity constraints. Renzini & Ciotti (1993) argued that the small scatter perpendicular to the FP implied a small age dispersion ($\leq 15\%$) and high formation redshift, fully consistent with the Bower et al. (1992) argument based on the narrowness of the Colour-Magnitude and colour- σ relations.

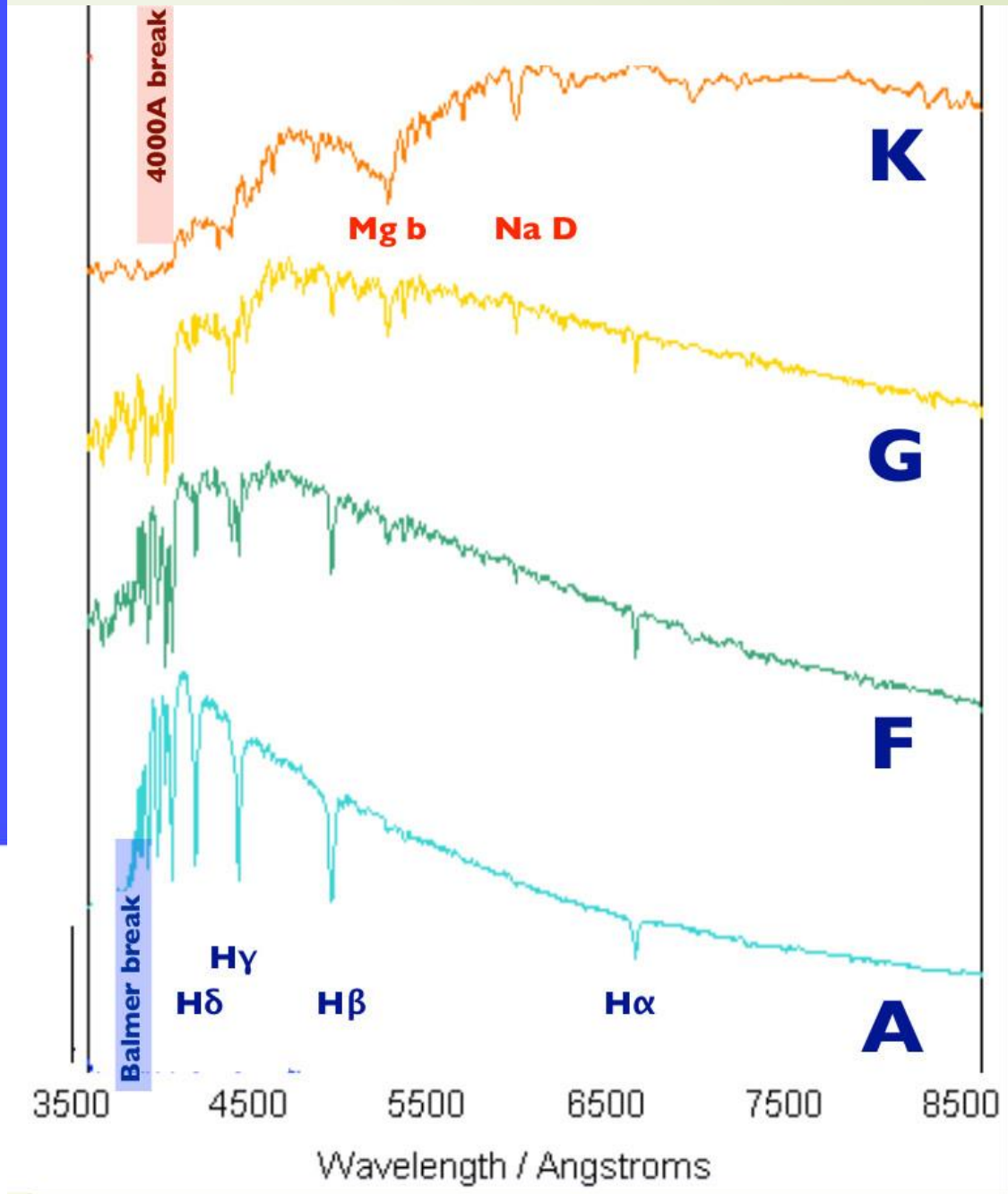
The line strength diagnostics. Lick indices

- Optical spectra of ETGs present a number of absorption features whose strength must depend on the distributions of stellar ages, metallicities, and abundance ratios.
- To exploit this opportunity, Burstein et al. (1984) introduced a set of indices now known as the Lick system. The most widely used indices have been the Mg_2 (or Mgb), Fe, and the $H\beta$ indices.



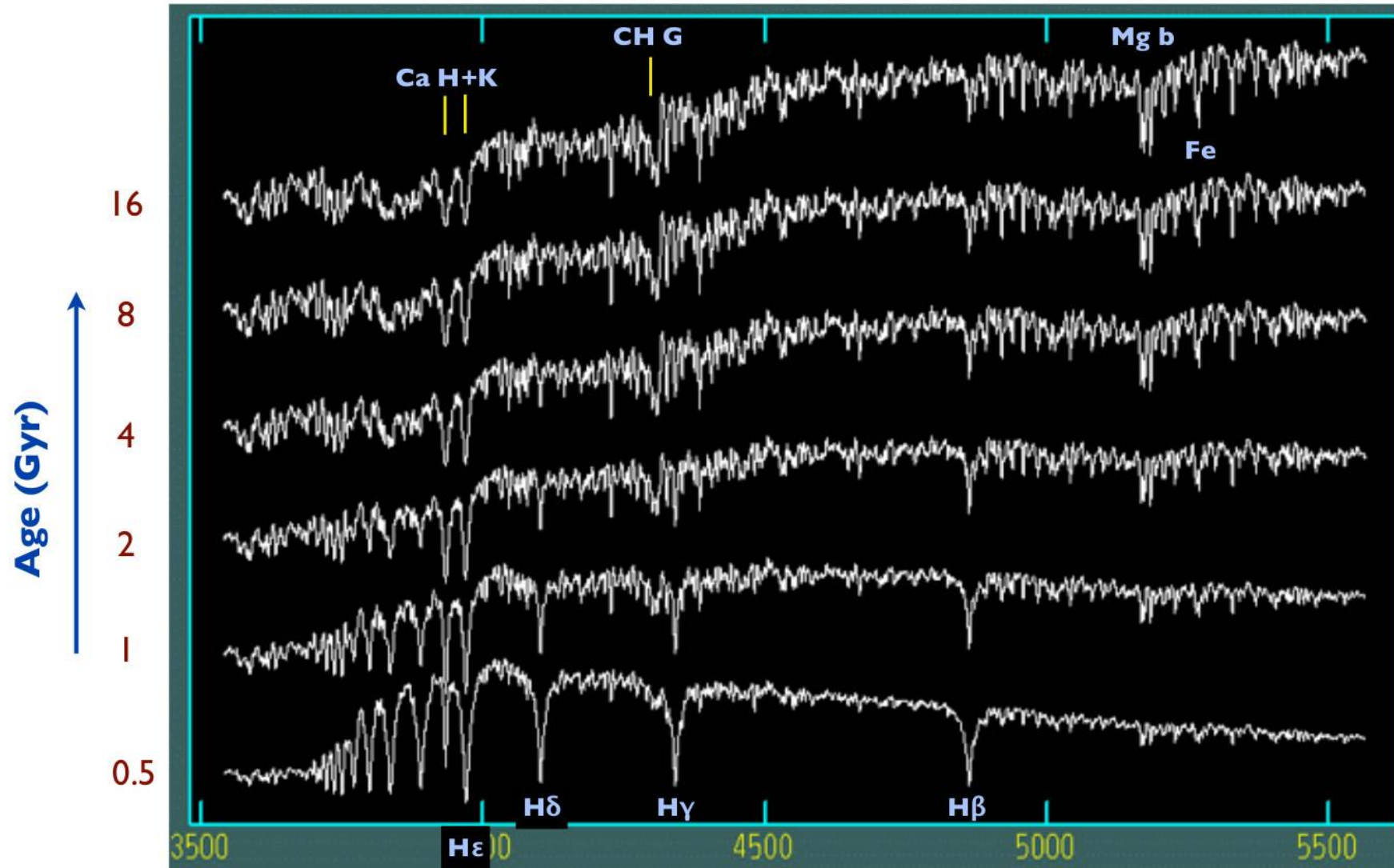
In particular note the increasing strength of Hydrogen lines (Balmer series) in the hotter stars.

These are strongest at spectral type A... which is why they were called "A"!



Source: R. Smith

SSP Spectra: Variation with Age

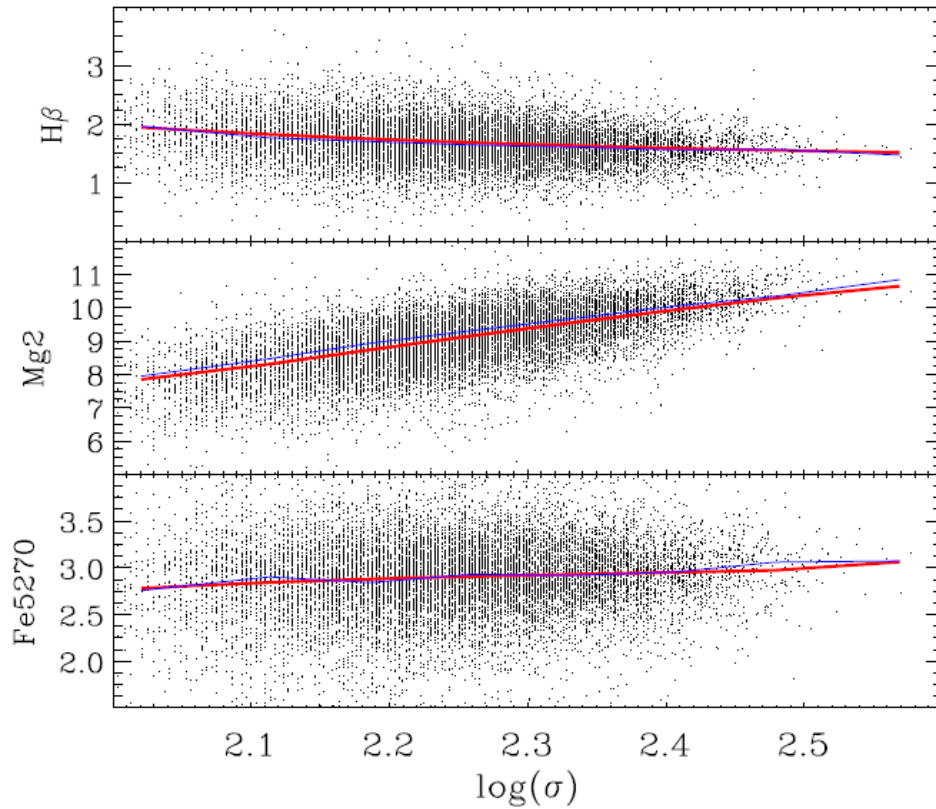


Vazdekis et al. (2010) models at solar Fe/H from MILES library.

Source: R. Smith https://www.astro.umd.edu/~richard/ASTRO620/stellarpops11_lec3.pdf

14000 ETGs $0.01 < z < 0.1$

*M.S. Clemens, A. Bressan,
B. Nikolic, Rampazzo 09*



$$\delta I =$$

$$\sum \left[\begin{array}{l} \frac{\partial I}{\partial \log(t)} \delta \log(t) \\ \frac{\partial I}{\partial \log(Z)} \delta \log(Z) \\ \frac{\partial I}{\partial [\alpha/Fe]} \delta [\alpha/Fe] \end{array} \right]$$

↑
Models

↓
Age, Z
[α/Fe]

Lick Indices (absorption strengths)

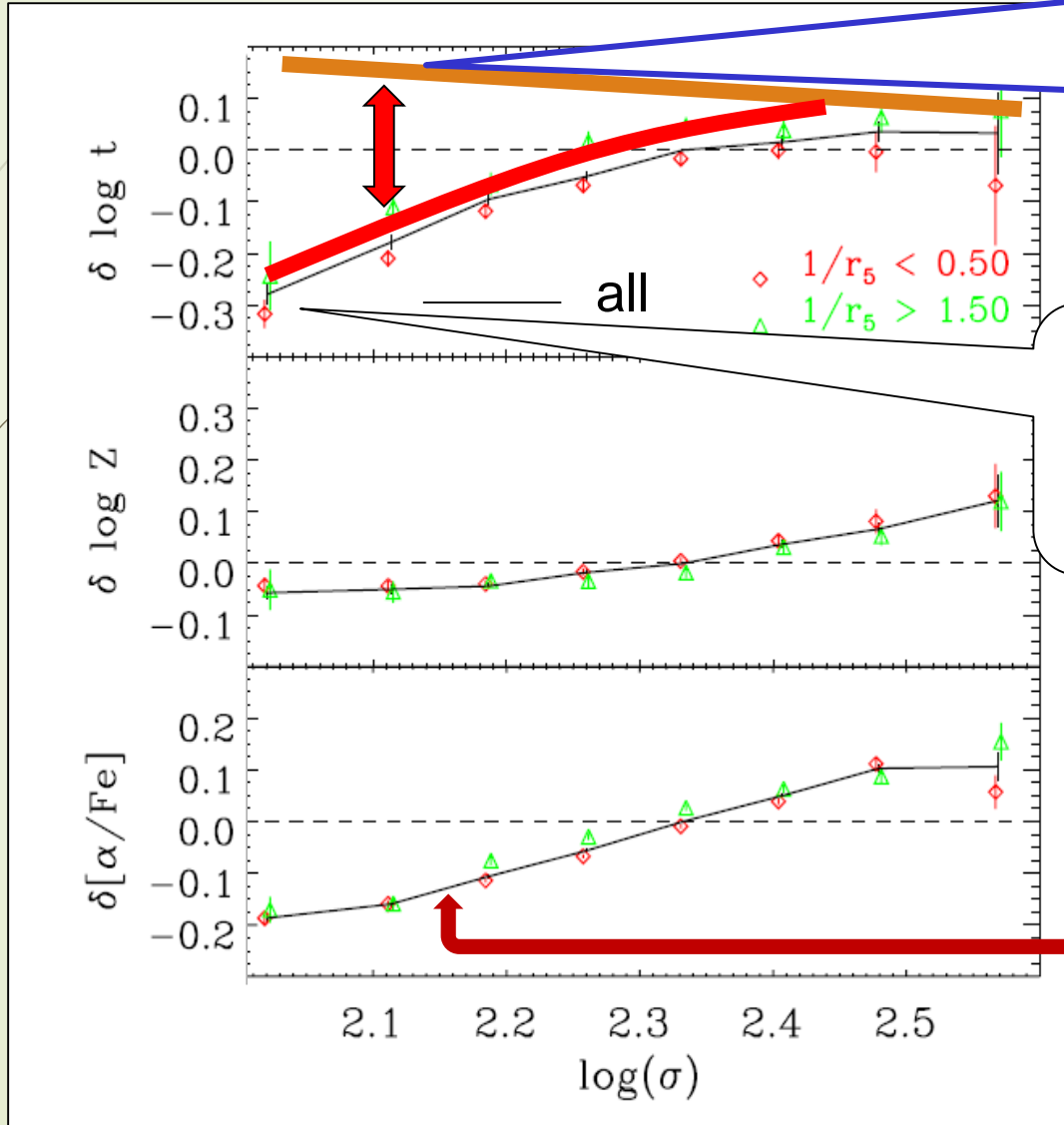
H β index: age sensitive

Star formation timescales of spheroidal galaxies - 1

- Models for the chemical evolution of elliptical show that the bulk of the Fe abundance is produced by type Ia SNe on a timescale of $\approx 10^9$ yr. The Fe enrichment is therefore delayed compared to α -elements, such as Mg, produced by type II SNe, on much shorter timescales ($\approx 10^8$ yr).
- The α -enhancement (high α /Fe ratio) observed in massive galaxies requires star formation timescales ≤ 0.5 -1 Gyr (Matteucci 1994; Thomas et al. 1999). This is at odds with earlier expectations of a decrease with increasing galactic mass of the [Mg/Fe] ratio, based on the assumption that the star formation timescale should be approximately equal to the dynamical timescale.

Formation of Early Type Galaxies

Clemens et al. (2009)



Evolution of DM Halos: smaller halos form first

In smaller galaxies star formation proceeds slowly

lower $[\alpha/\text{Fe}]$ indicates longer duration

r_5 = distance to the fifth nearest neighbour

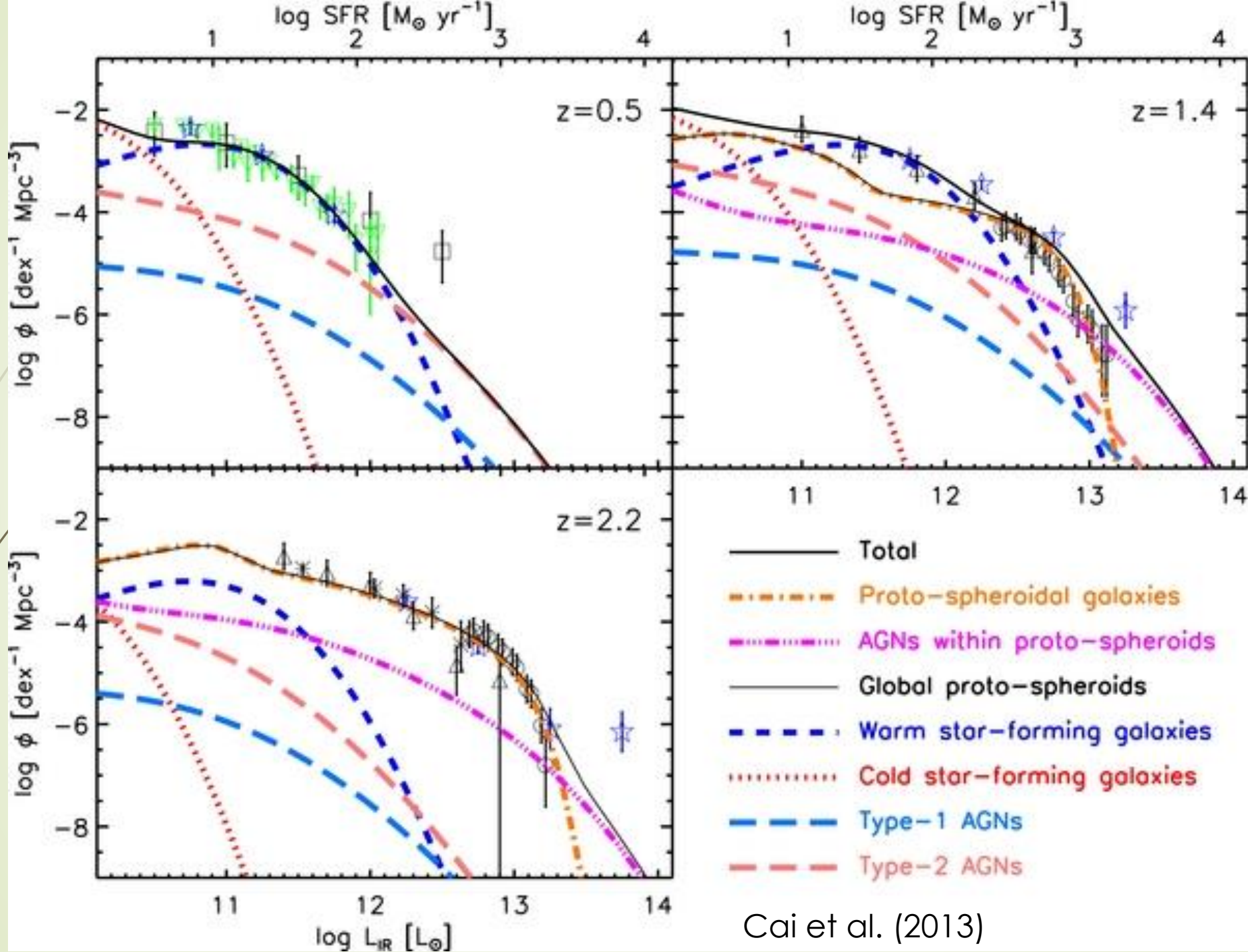
Star formation timescales of spheroidal galaxies - 2

- ▶ Another constraint on the star-formation timescale for Early Type Galaxies (ETGs) comes from the luminosity functions of sub-mm galaxies, determined up to $z \approx 4$ from Herschel survey data (Eales et al. 2010; Lapi et al. 2011; Gruppioni et al. 2014).
- ▶ The comoving density of galaxies with given SFR or infrared luminosity at redshift z is related to the density of host halos by

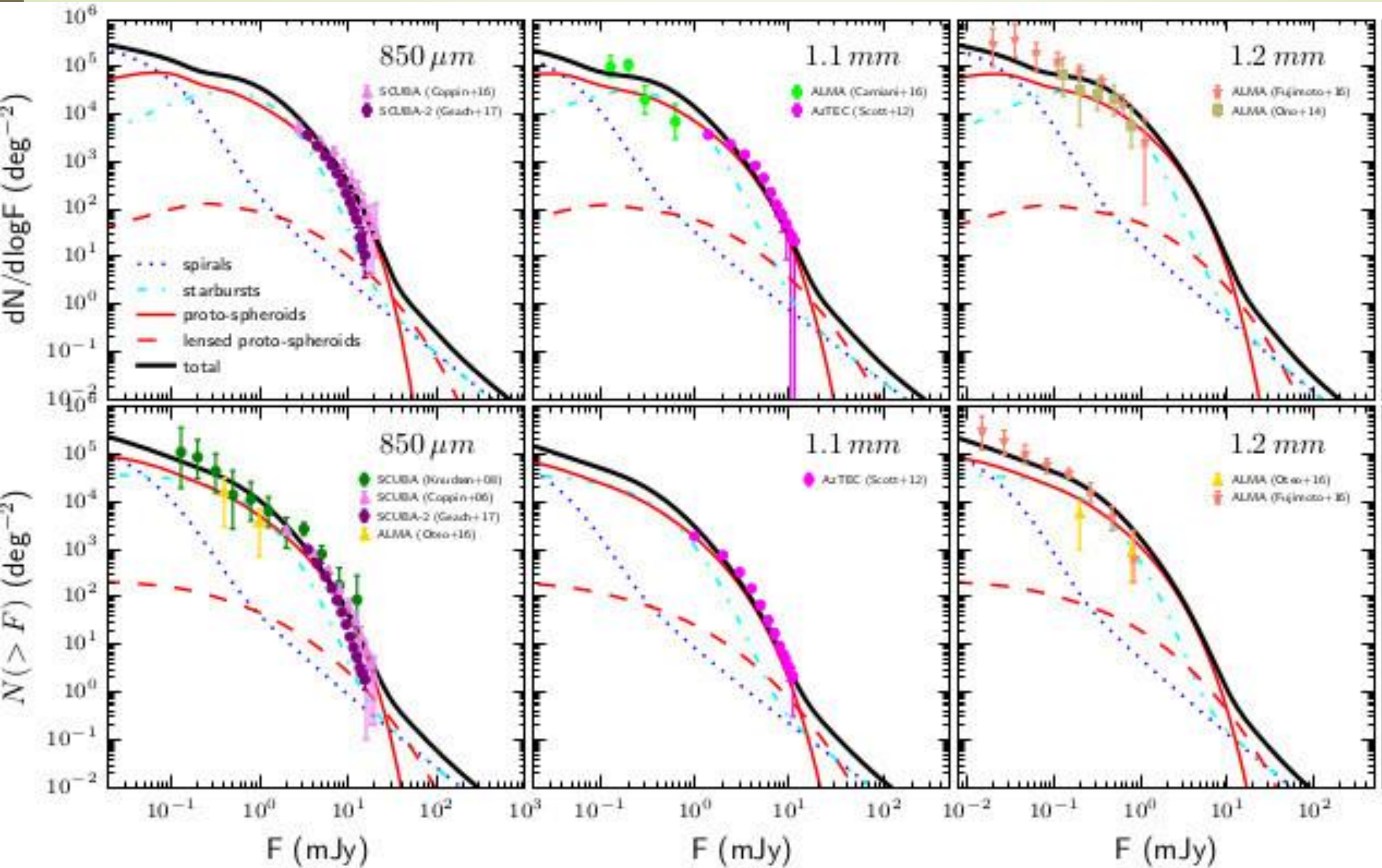
$$\Phi(SFR, z) \sim N(M_h, z) \frac{t_{SFR}}{\tau_{exp}}$$

where τ_{exp} is the age of the universe at z and τ_{SFR} is the lifetime of the star forming phase.

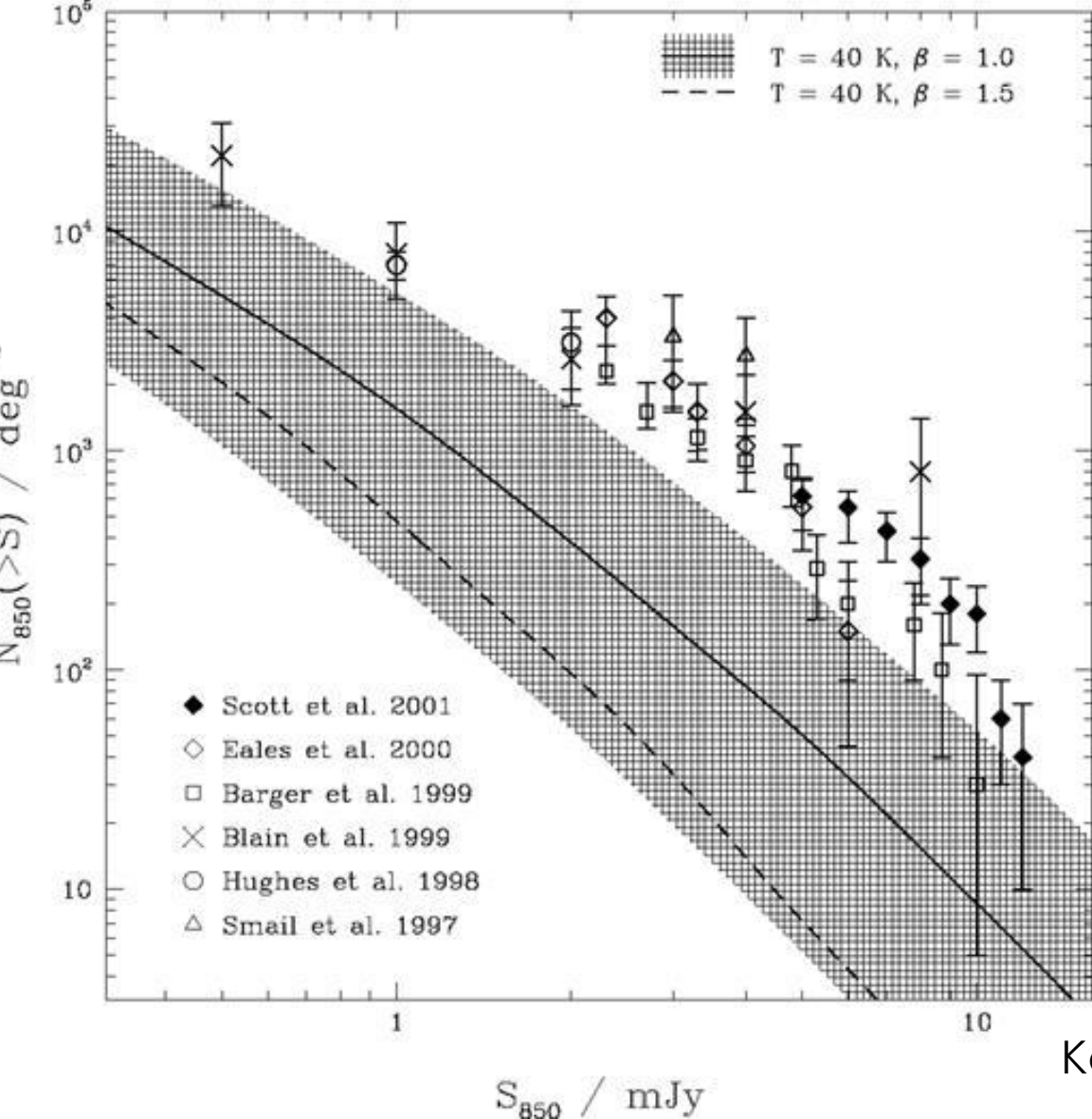
- ▶ Observational determinations of $\Phi(SFR, z)$ are matched by typical $\tau_{SFR} \approx 0.7$ Gyr for the most massive galaxies, increasing with decreasing mass.



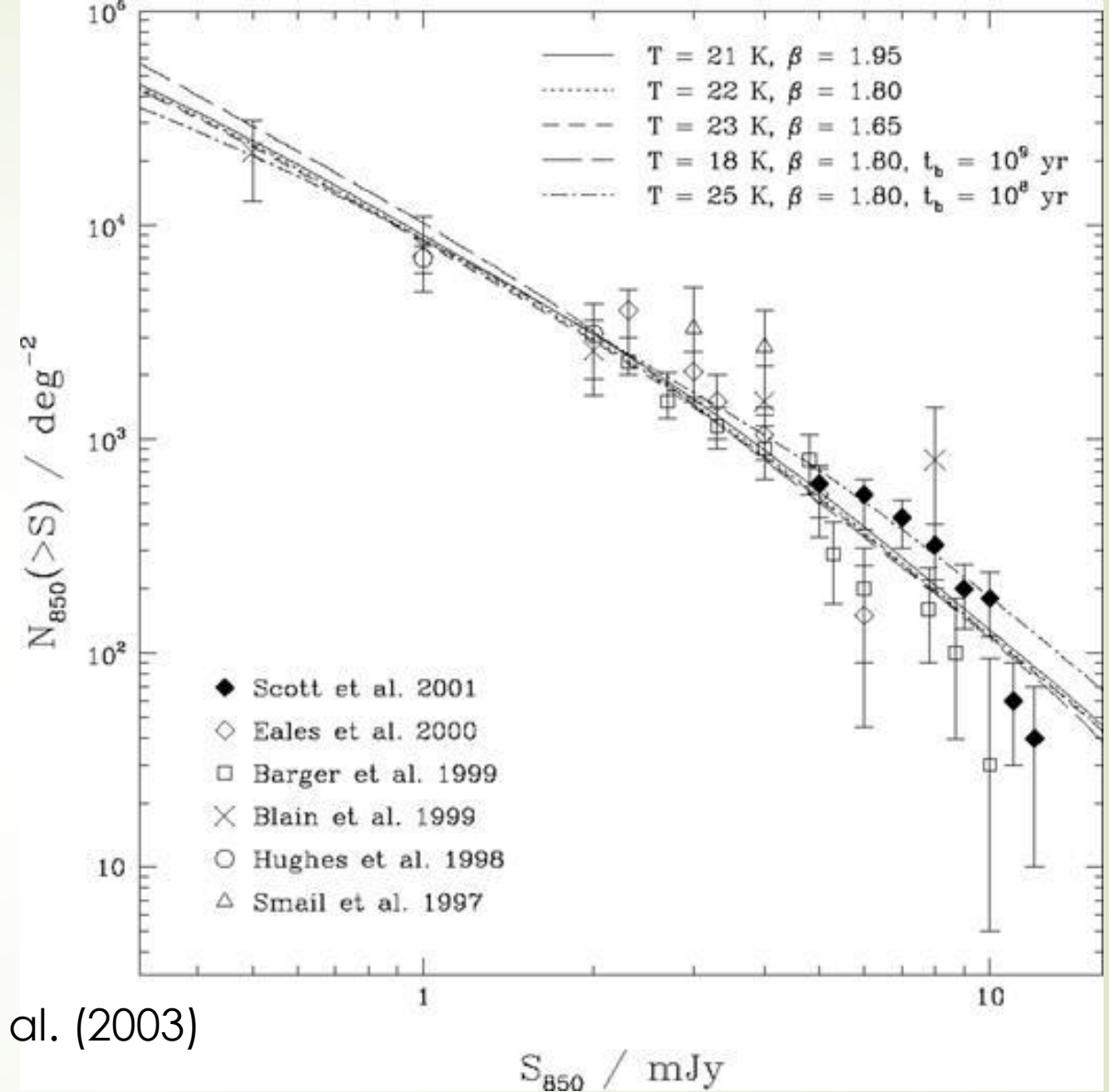
Cai et al. (2013)



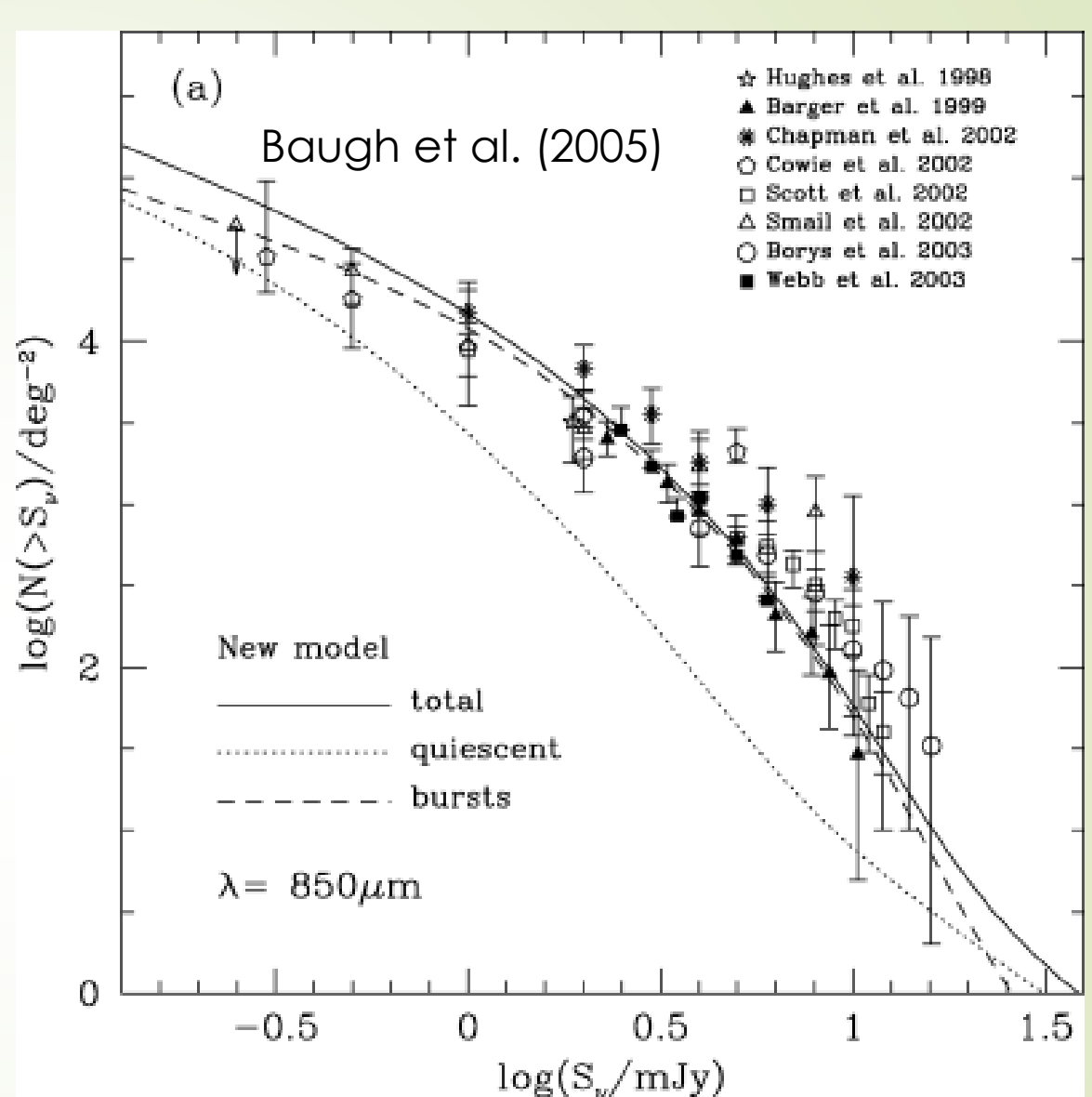
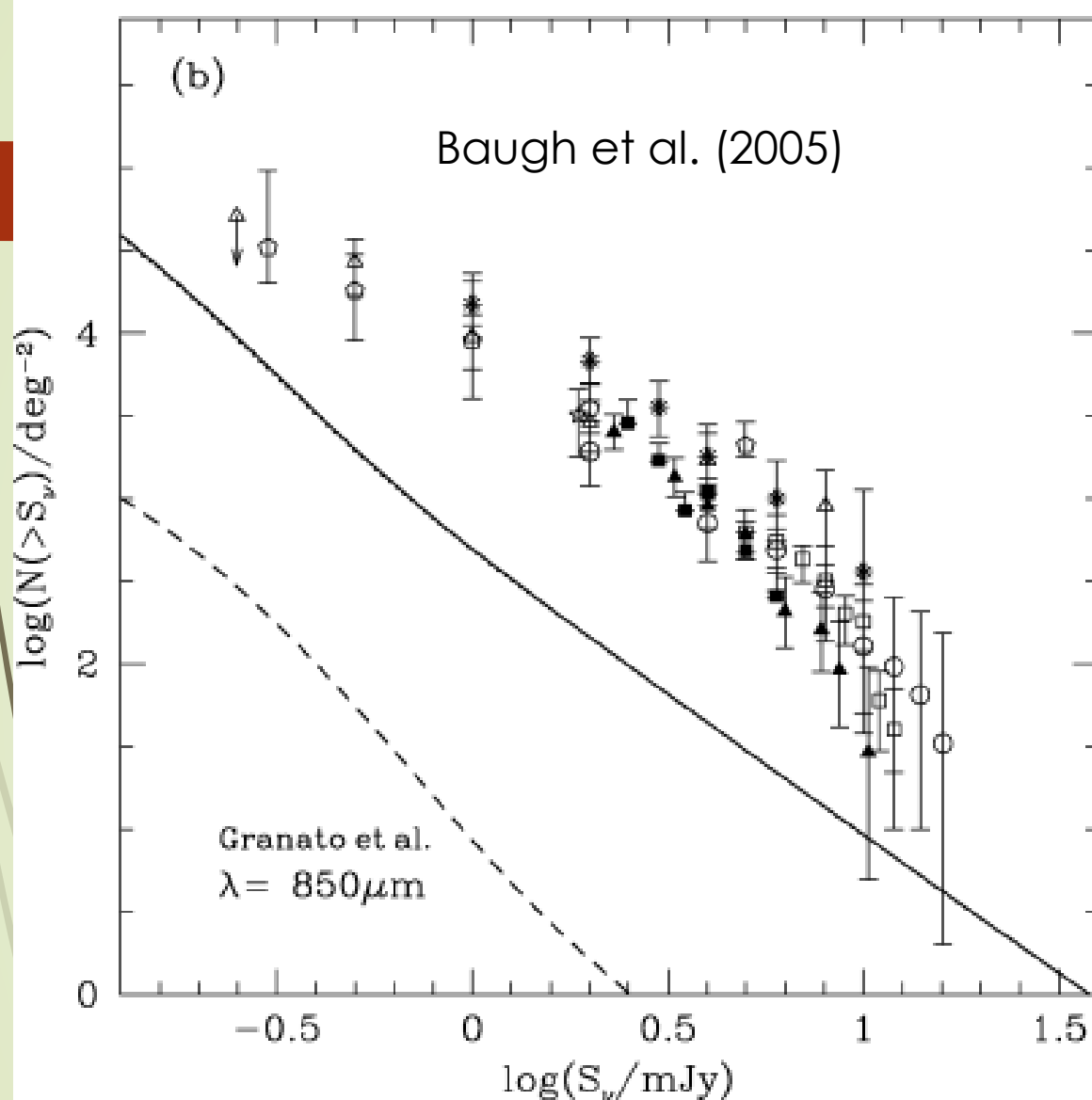
Cai et al. (2013) model. Figure: courtesy of M. Negrello



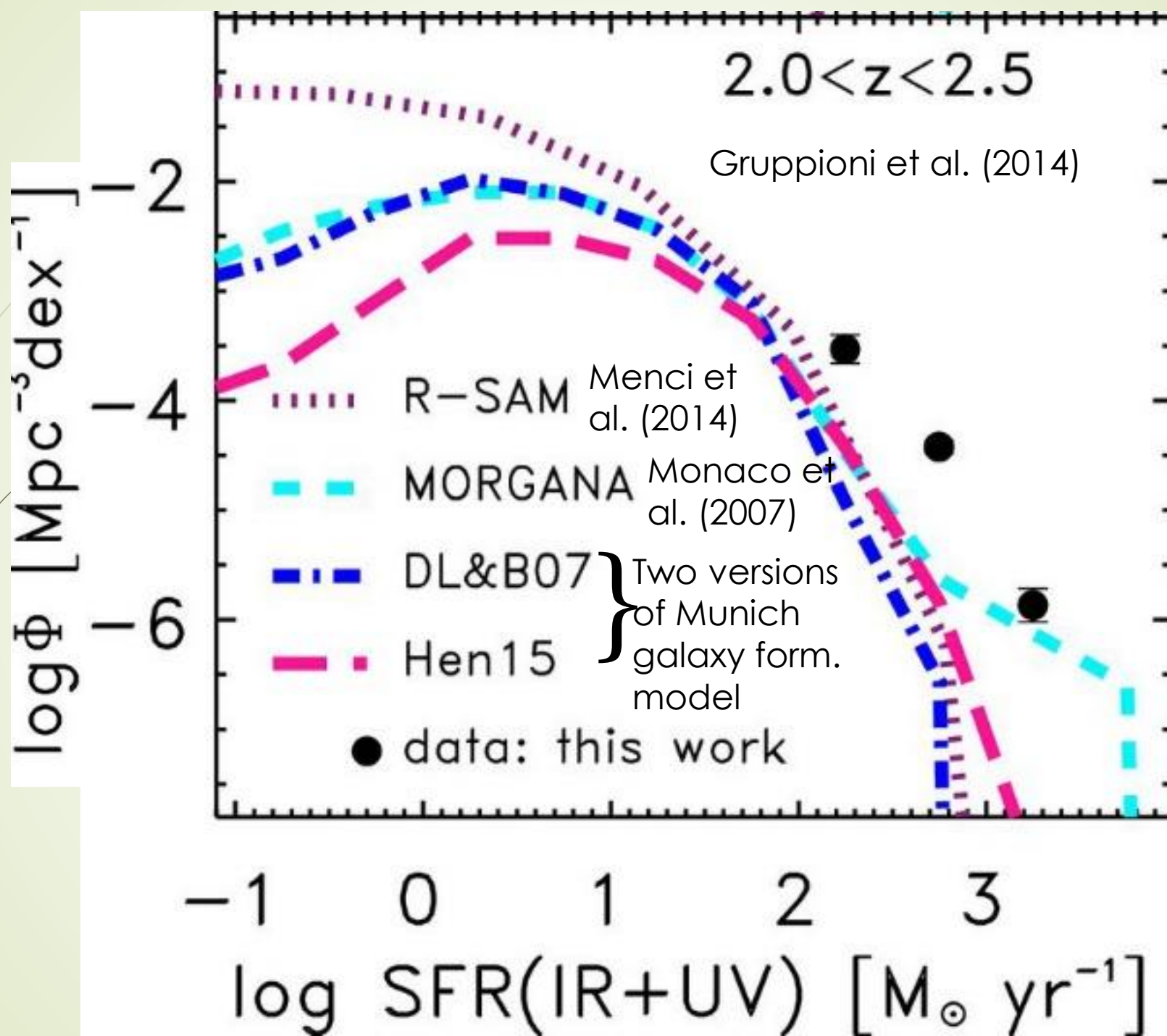
Kaviani et al. (2003)



To recover agreement with the observed counts it was necessary to assume dust temperatures $\sim 20 \text{ K}$, much lower than those expected, and actually observed, for the compact high- z sub-mm galaxies (30-40 K). Lower temperatures shift power to longer wavelengths. This solution is inconsistent with counts at shorter wavelengths.



The early predictions of the Durham model (Granato et al. 2000; left panel) were orders of magnitude lower than the observed $850\mu\text{m}$ counts. To recover agreement, Baugh et al. (2005) made several modifications, the most important of which was the adoption of a top-heavy (i.e., flat, $dN/d \ln m = \text{const}$) IMF in bursts. Such a flat IMF has no observational confirmation. Also it makes difficult to account for the galaxy main sequence.



Constraints from clustering

- An important constraint on any evolutionary picture comes from observational measurements of the clustering of selected galaxies, which provides information on the masses of the dark matter haloes in which they reside.
- However, measuring the clustering of FIR/sub-mm galaxies has proven challenging.
- Information about the clustering, and therefore host halo masses, of the unresolved FIR/sub-mm galaxies which contribute to the bulk of the Cosmic Infrared Background (CIB), can be obtained from the angular power spectrum of CIB anisotropies.
- A clear signal has been measured on Herschel and Planck maps (Viero et al. 2013; Planck Collaboration XXX 2014).
- The Viero et al. and the Planck Collaboration studies infer the typical halo mass for galaxies that dominate the CIB power spectrum as $10^{11.95 \pm 0.5} h^{-1} M_{\odot}$ and $10^{12.43 \pm 0.1} h^{-1} M_{\odot}$, respectively, making various assumptions.

Galaxy Biasing

Suppose that the density fluctuations in mass and in light are not the same, but

Or:

$$(\Delta\rho/\rho)_{light} = b (\Delta\rho/\rho)_{mass}$$
$$\xi(r)_{light} = b^2 \xi(r)_{mass}$$

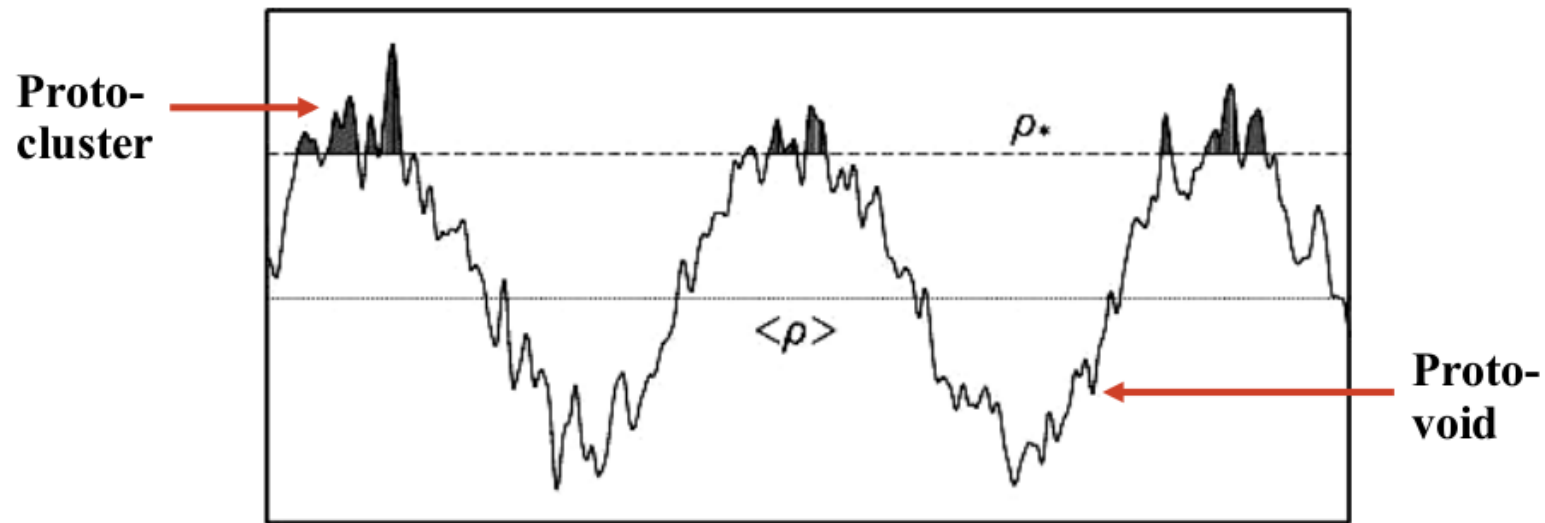
Here b is the *bias factor*.

If $b = 1$, light traces mass exactly (this is indeed the case at $z \sim 0$, at scales larger than the individual galaxy halos). If $b > 1$, light is a *biased tracer* of mass.

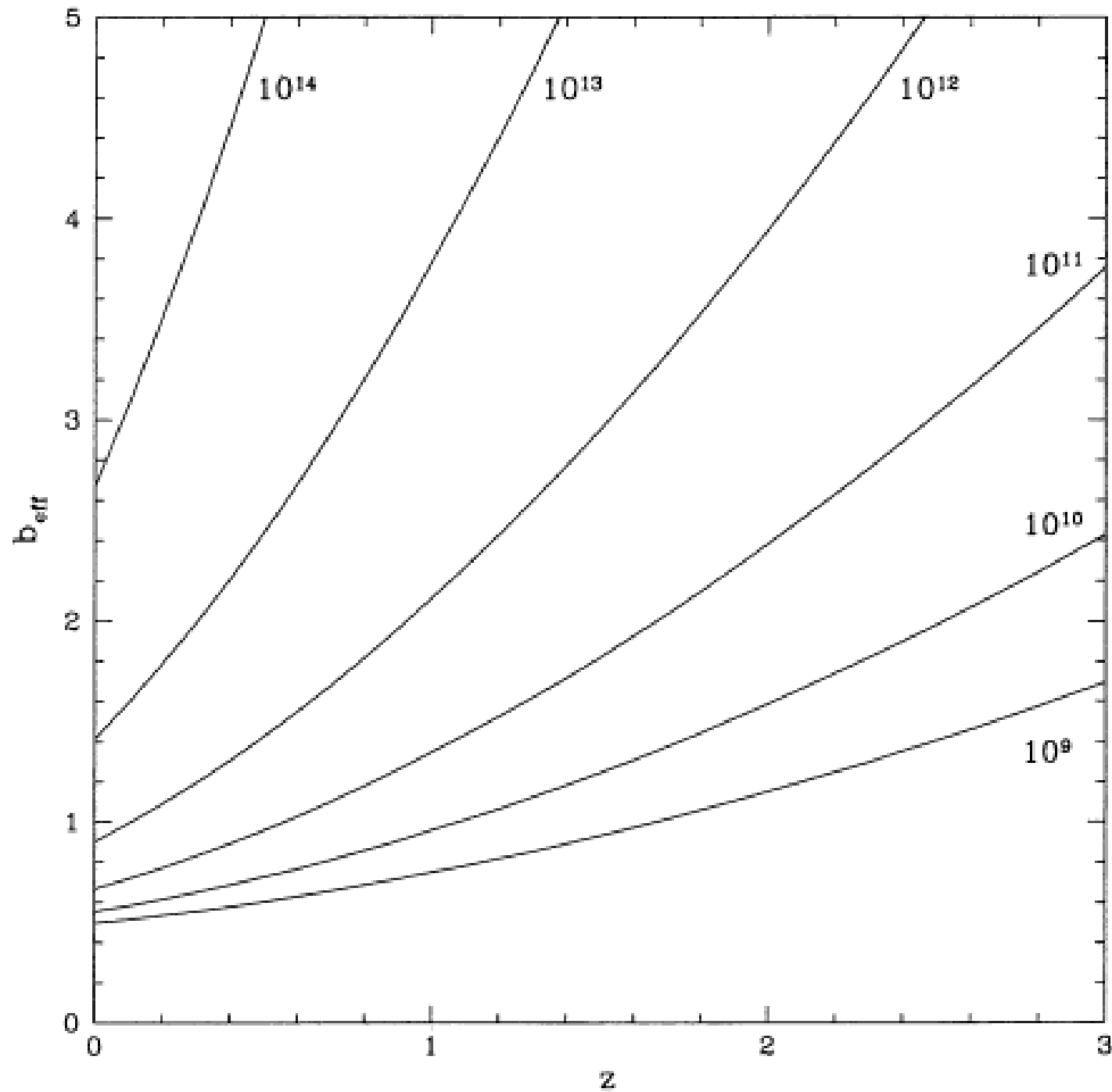
One possible mechanism for this is if the galaxies form at the densest spots, i.e., the highest peaks of the density field. Then, density fluctuations containing galaxies would not be typical, but rather a biased representation of the underlying mass density field; if 1- σ fluctuations are typical, 5- σ ones certainly are not.

High Density Peaks as Biased Tracers

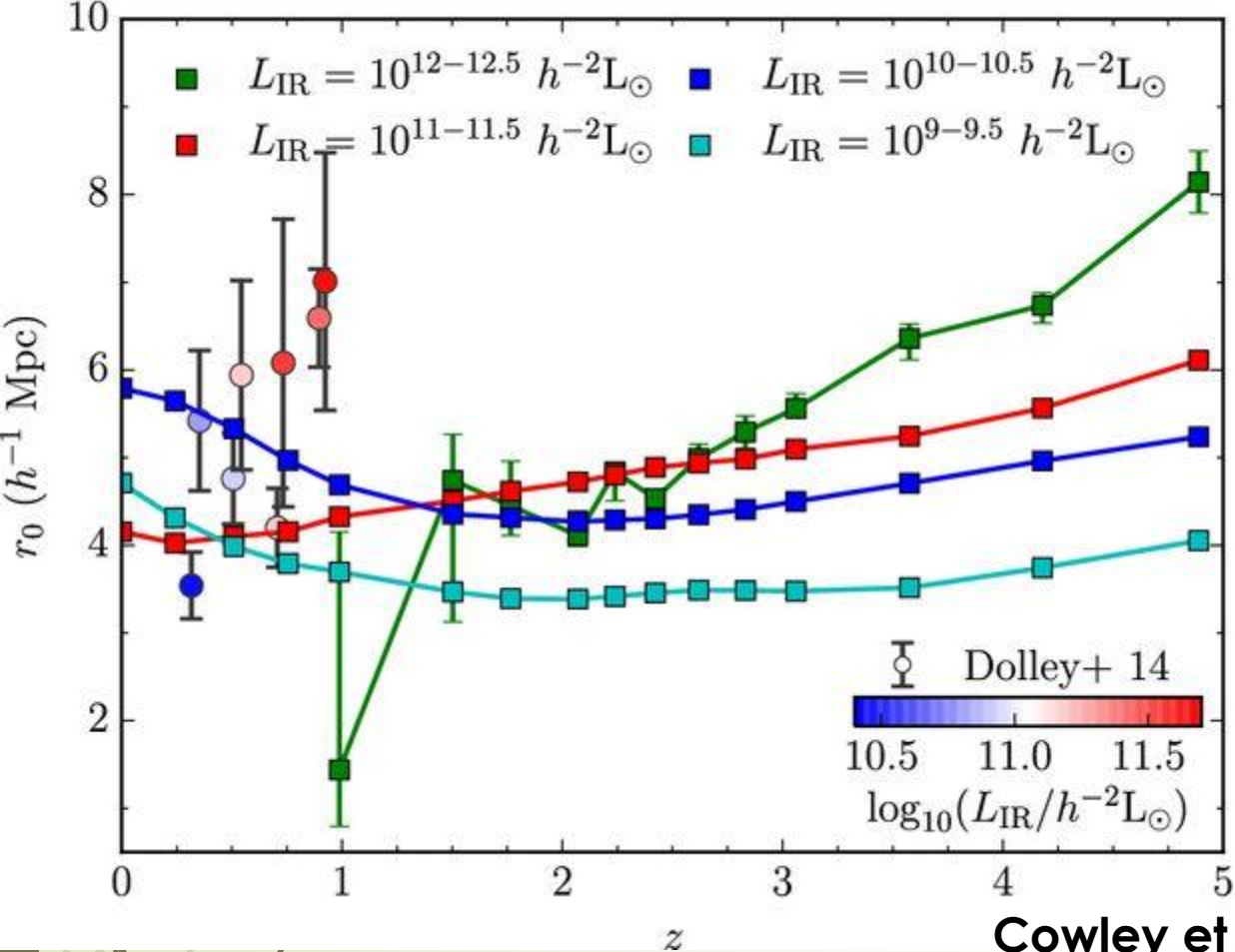
Take a cut through a density field. Smaller fluctuations ride atop of the larger density waves, which lift them up in bunches; thus the highest peaks (densest fluctuations) are a priori clustered more strongly than the average ones:



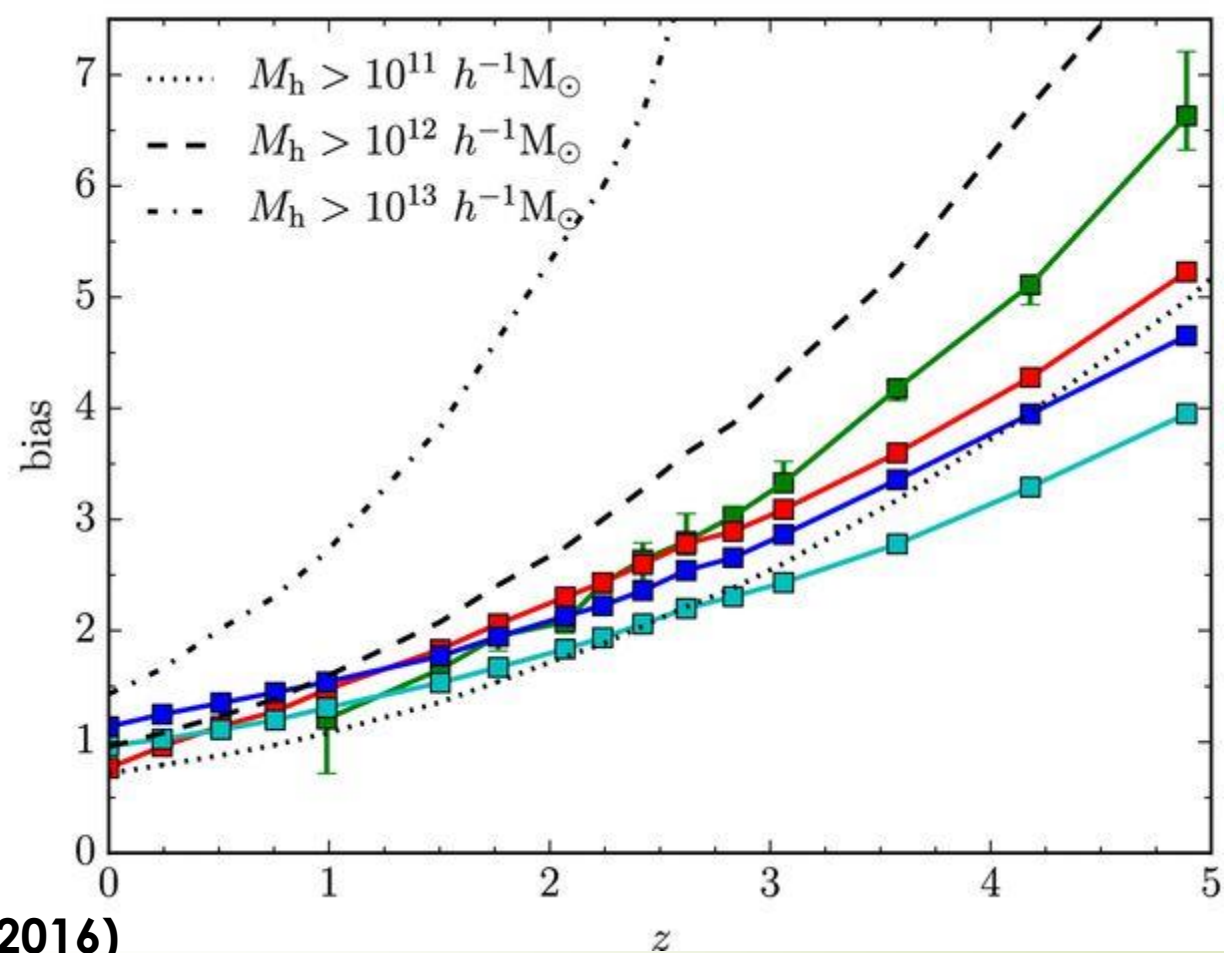
Thus, if the first galaxies form in the densest spots, they will be strongly clustered, but these will be very special regions.



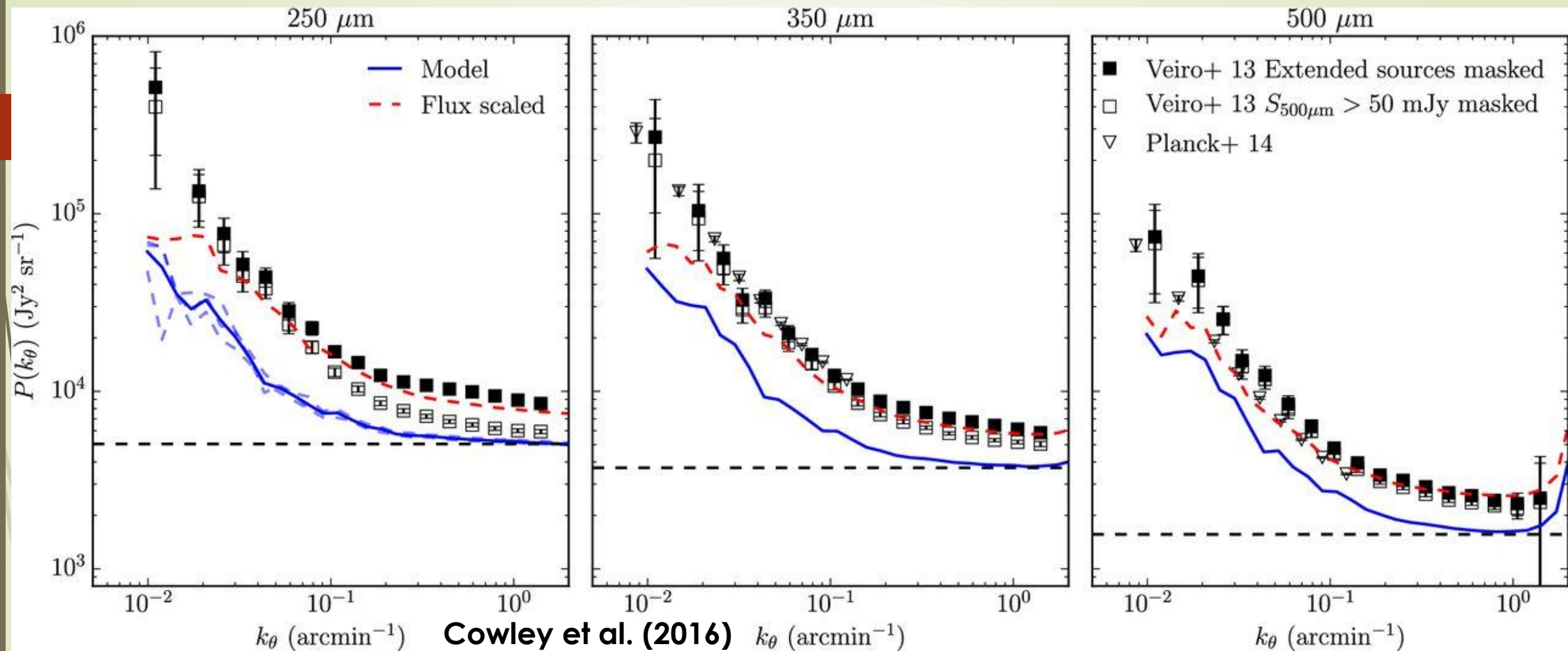
Effective bias as a function of redshift for different halo masses. At any z , b_{eff} is a strong function of M_h and therefore provides an estimate of the halo mass. From Matarrese et al. (1997).



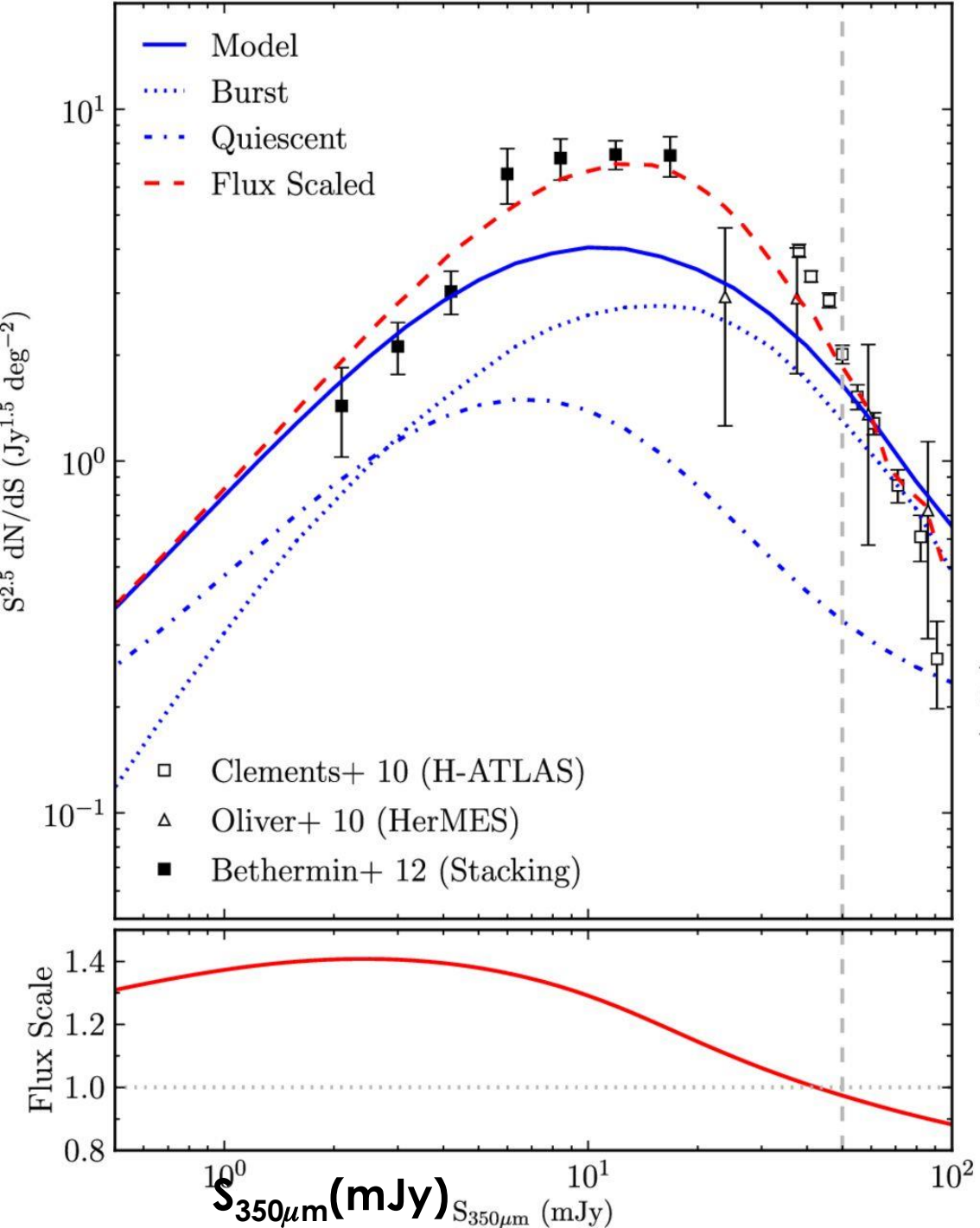
Cowley et al. (2016)



Left-hand panel: evolution of the comoving correlation length r_0 [defined such that $\xi(r_0) \equiv 1$]. The errors indicate 1σ volume bootstrap errors for the $L_{\text{IR}} = 10^{12}-10^{12.5}h^{-2}L_{\odot}$ population. A selection of observational estimates from Dolley et al. (2014) are shown as circles, with the colour scale indicating the mean L_{IR} for each sample, as shown on the inset colour bar. Right-hand panel: as for the left-hand panel, but indicating the evolution of the large-scale bias. The dotted, dashed and dash-dotted lines indicate the bias evolution for haloes of $M_h > 10^{11}$, 10^{12} and $10^{13}h^{-1}M_{\odot}$ respectively. GALFORM code (Durham)

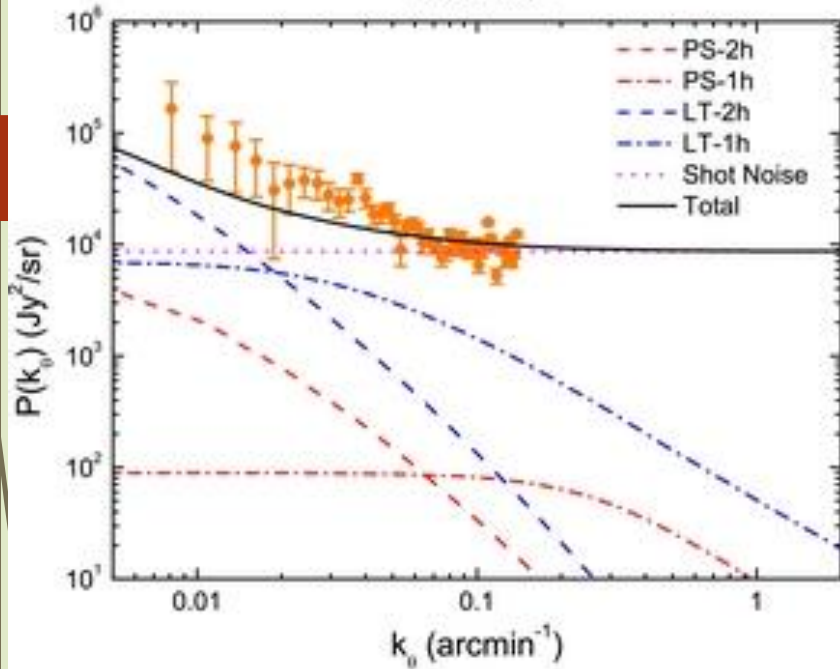


Angular power spectra of CIB anisotropies predicted by our model at 250, 350 and 500 μm (left- to right-hand panels). The blue solid line indicates the power spectrum averaged over three randomly orientated lightcones, each with an area of 20 deg^2 . The dashed blue lines in the left-hand panel indicate the power spectra for each of these fields individually. The horizontal dashed line shows the predicted shot noise contribution to power spectra. The dashed red line shows the prediction of our model after the fluxes of our simulated galaxies have been rescaled (see text). We compare to the observational data of Veiro et al. (2013, squares) with the filled and open squares corresponding to different levels of masking, and to that of the Planck Collaboration XXX (2014, triangles).

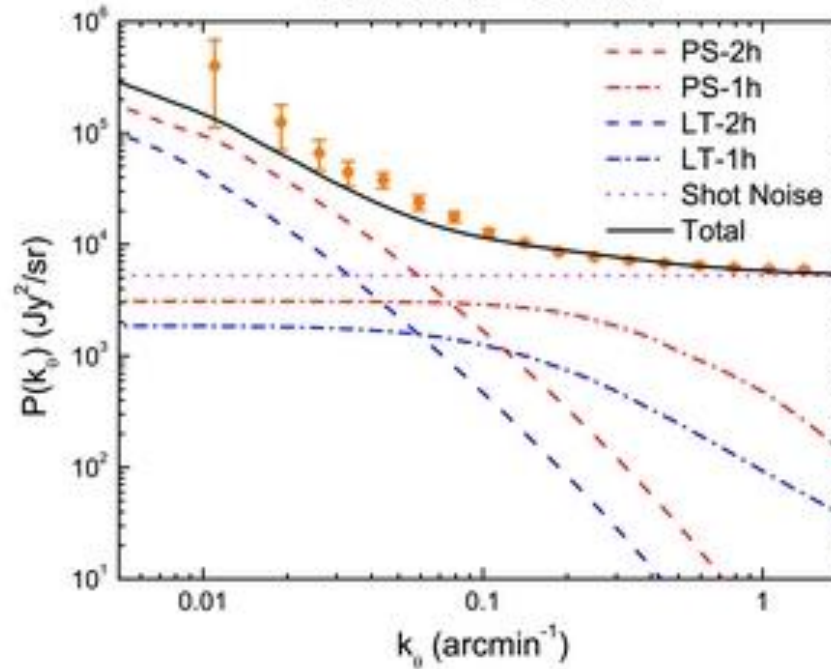


An example of flux re-scaling scheme at $350 \mu\text{m}$. Top panel: predicted number counts (blue line) showing the contribution to the counts from starburst and quiescent galaxies (dotted and dot-dashed lines, respectively). The red dashed line shows the number counts after the flux rescaling has been applied. Bottom panel: the flux rescaling applied to simulated galaxies as a function of original model flux. A horizontal dotted line is drawn at unity for reference. The vertical dashed line in both panels indicates a flux of 50 mJy , the limit brighter than which galaxies are not included in the power spectrum estimate in order to match the masking applied by Viero et al. (2013). From Cowley et al. (2016).

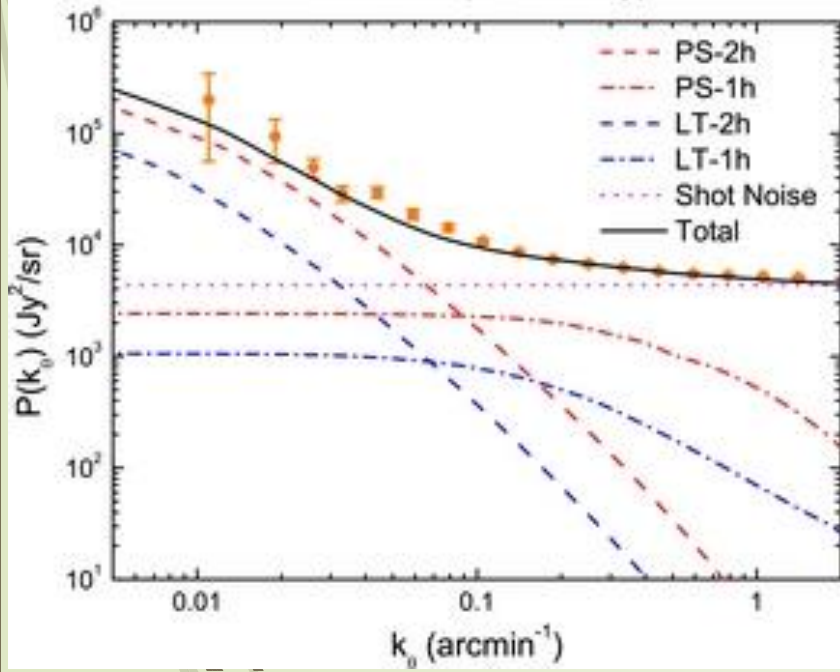
100 x 100



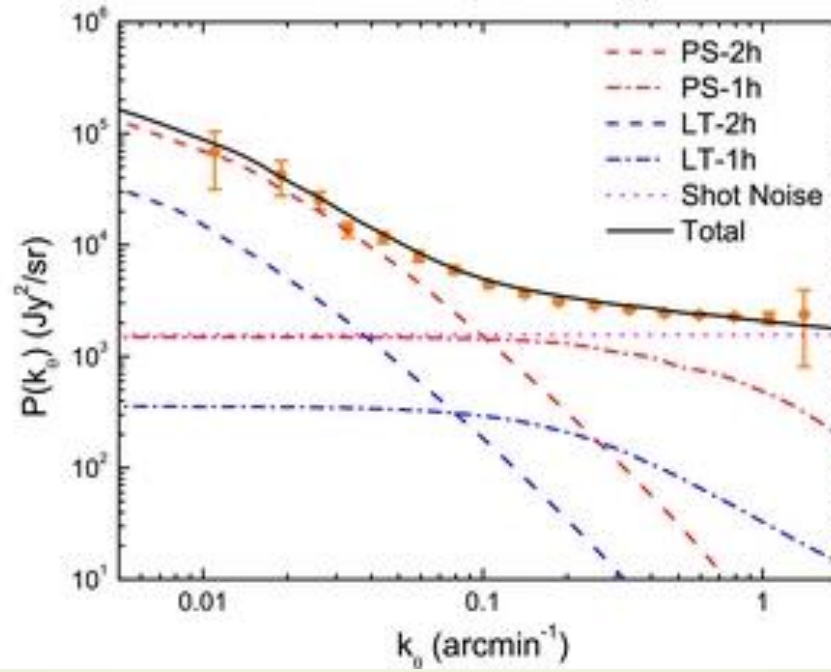
250 x 250 (S > 50 mJy)



350 x 350 (S > 50 mJy)



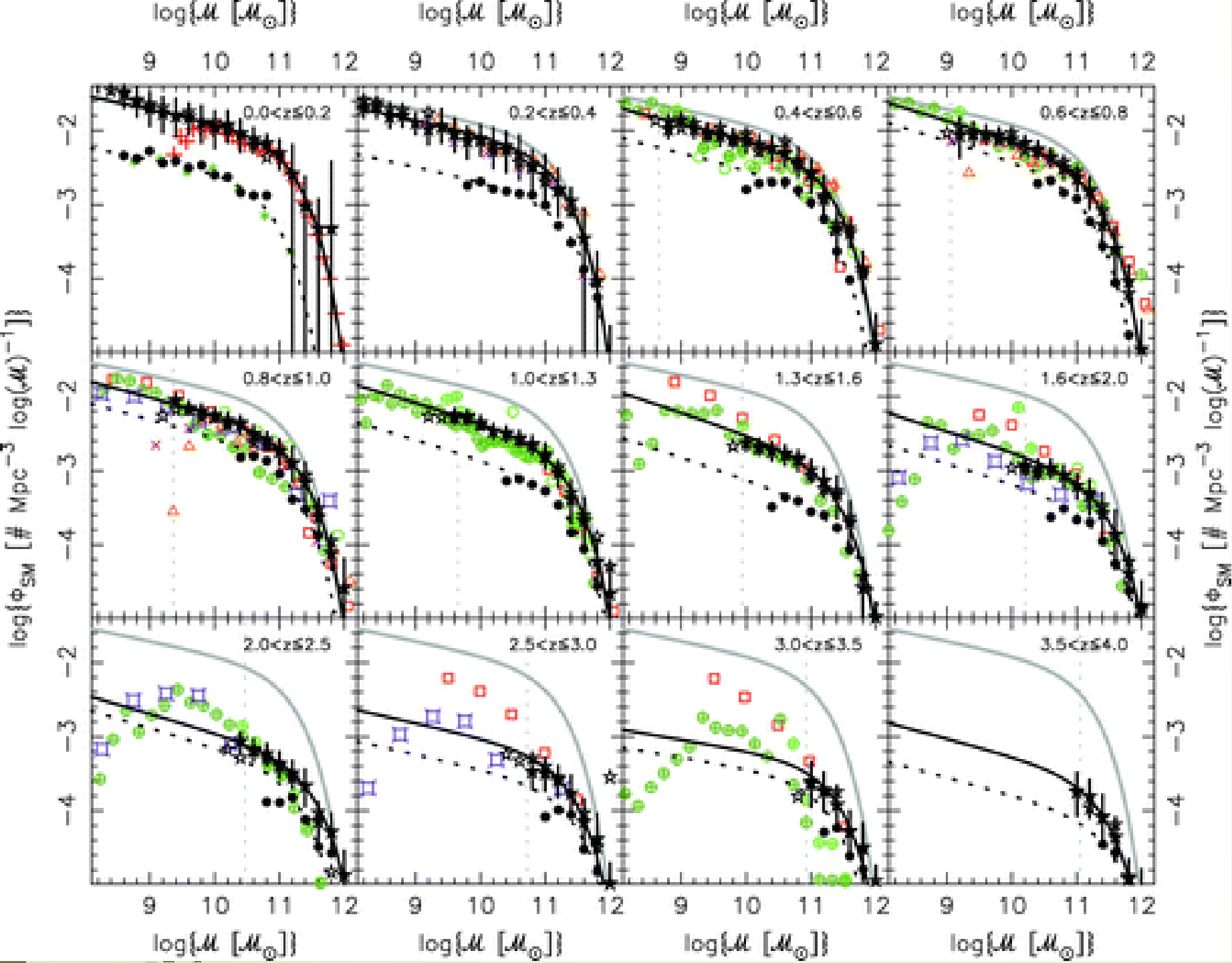
500 x 500 (S > 50 mJy)



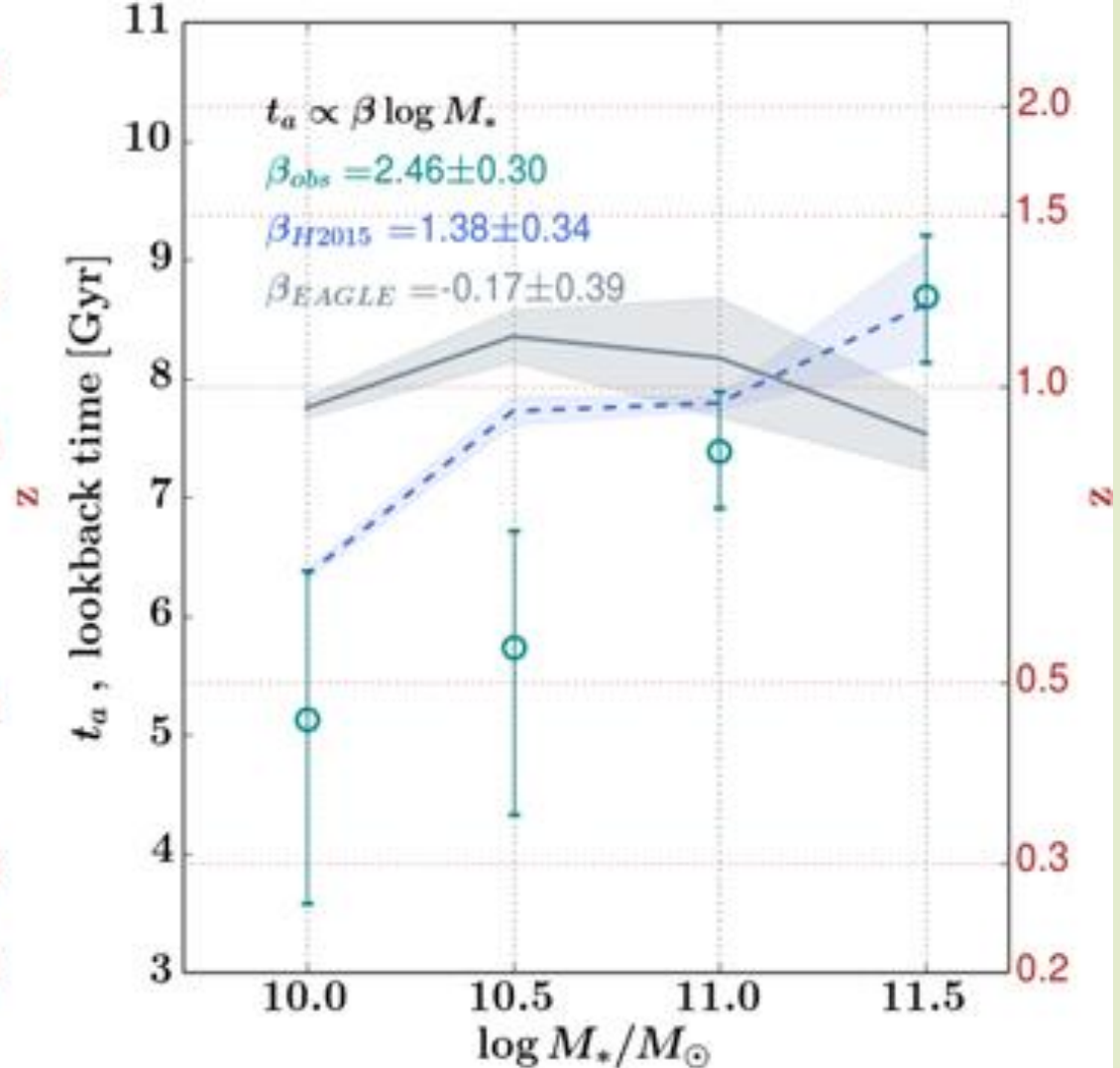
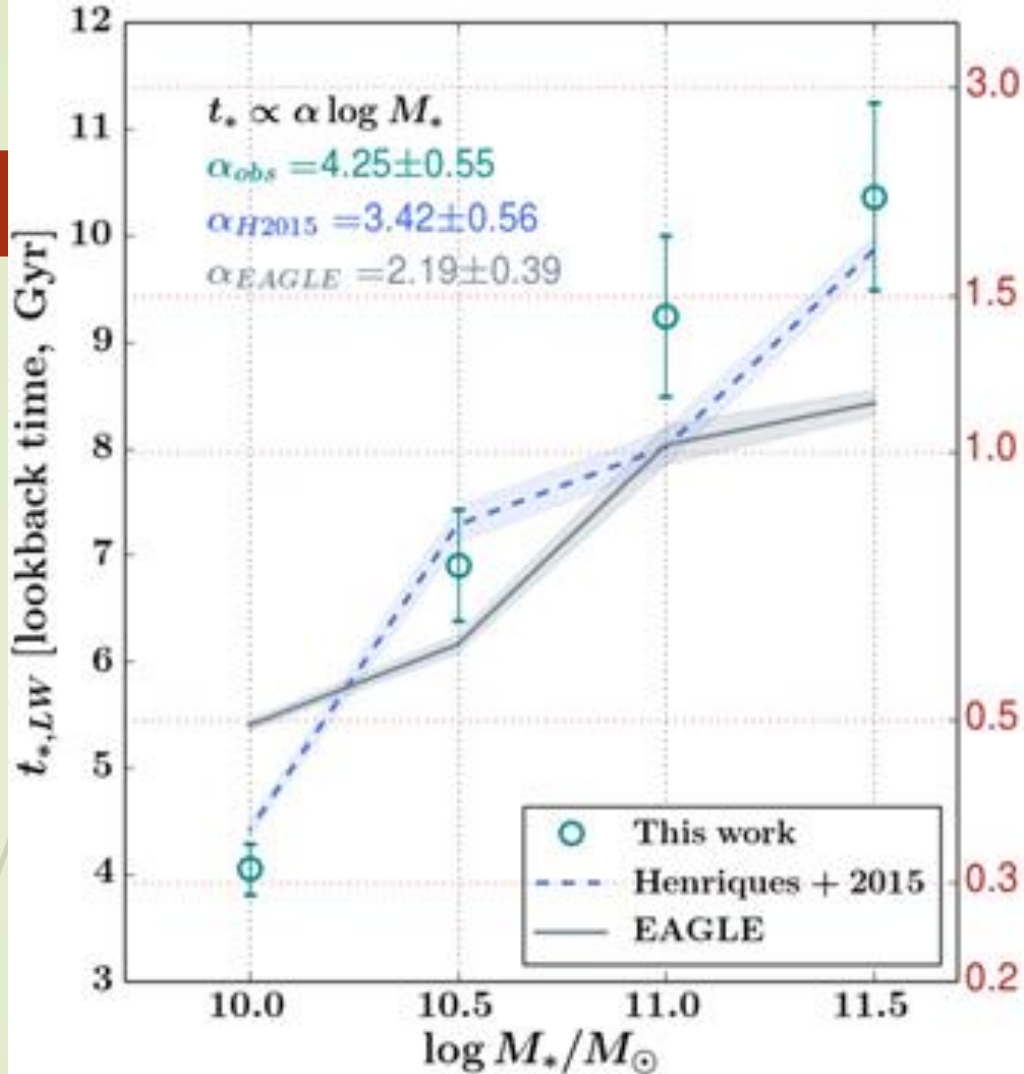
The clustering data can be accounted for with durations of the star-forming phase ~ 0.7 Gyr for the most massive halos, increasing with decreasing halo mass. Figure from Cai et al. (2013).

Galaxy downsizing

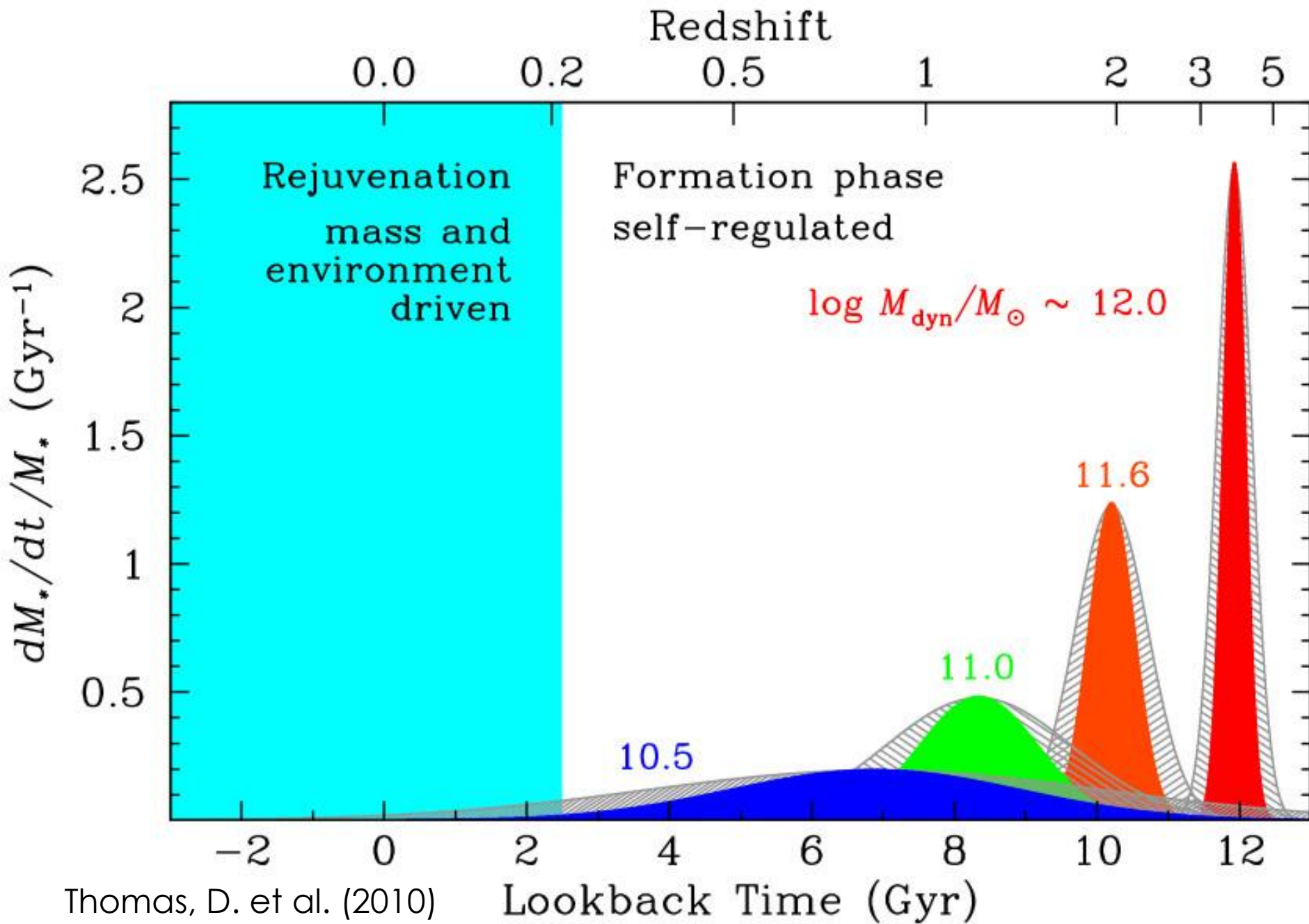
- ▶ Prior to 2000 or so, the widely accepted hierarchical galaxy formation models predicted that small galaxies form prior to massive galaxies.
- ▶ However it had long been known that observations were presenting a very different view. The first indications that this was in error came from the recognition that more massive early-type galaxies have redder colors (de Vaucouleurs 1961), higher metallicities (Faber 1973) and enhanced $[\alpha]/[\text{Fe}]$ metallicity ratios (Ziegler et al. 2005), indicative of an older stellar population with a shorter star formation time. This effect is called **downsizing**, as the most massive galaxies have their stellar populations in place early. assembly favored more massive systems at earlier epochs.
- ▶ A direct view of galaxy downsizing comes from determinations of the redshift-dependent stellar mass function.



Evolution of the stellar mass functions from $z=0$ to 4. Symbols refer to different observational determinations. The SMF data are fitted with a Schechter (1976) function (solid black line for the global SMF, and dashed line for the SMF for 24 μm sources). All panels show the local SMF from Cole et al. (2001) with a gray curve. From Pérez-González et al. (2008).



Stellar age (left) and assembly age (right) as function of the final stellar masses. The turquoise circles are the values determined from observations of the galaxy mass functions, solid gray lines are median values from the EAGLE simulation (Schaye et al. 2015), and dashed blue lines are from the SAM of Henriques et al. (2015; H2015). with the shaded regions around these lines representing the error. From Hill et al. (2017)



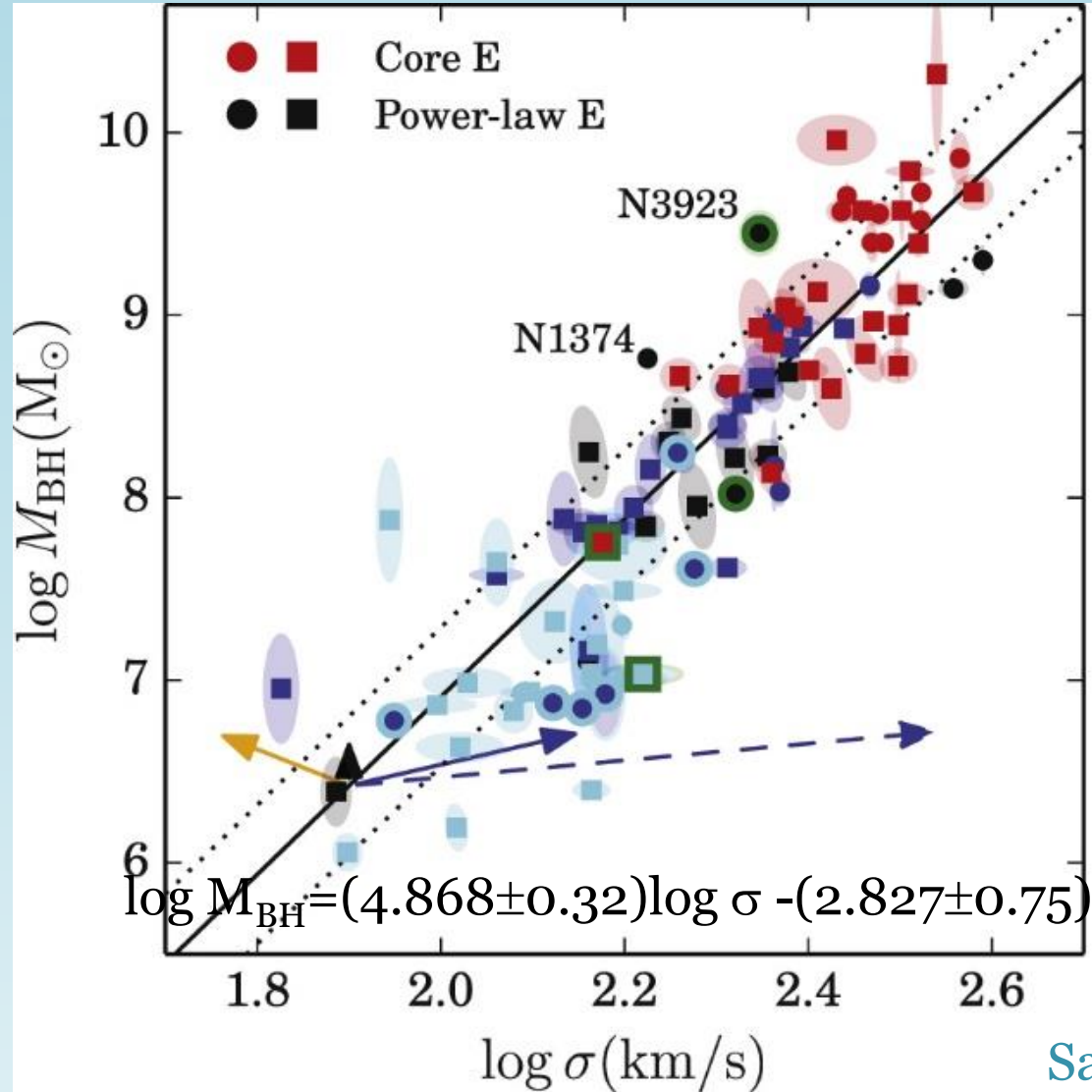
Thomas, D. et al. (2010)

Typical specific star formation rate history, as function of look-back time for ETGs of various masses, averaged over the entire galaxy population (at a given mass). The grey hatched curves indicate the range of possible variation in the formation time-scales allowed within the intrinsic scatter of the α/Fe ratios. Intermediate- and low-mass galaxies get rejuvenated via minor star formation. This suggests a transition from a self-regulated formation phase to a rejuvenation phase, in which the environment plays a decisive role possibly through galaxy mergers and interactions

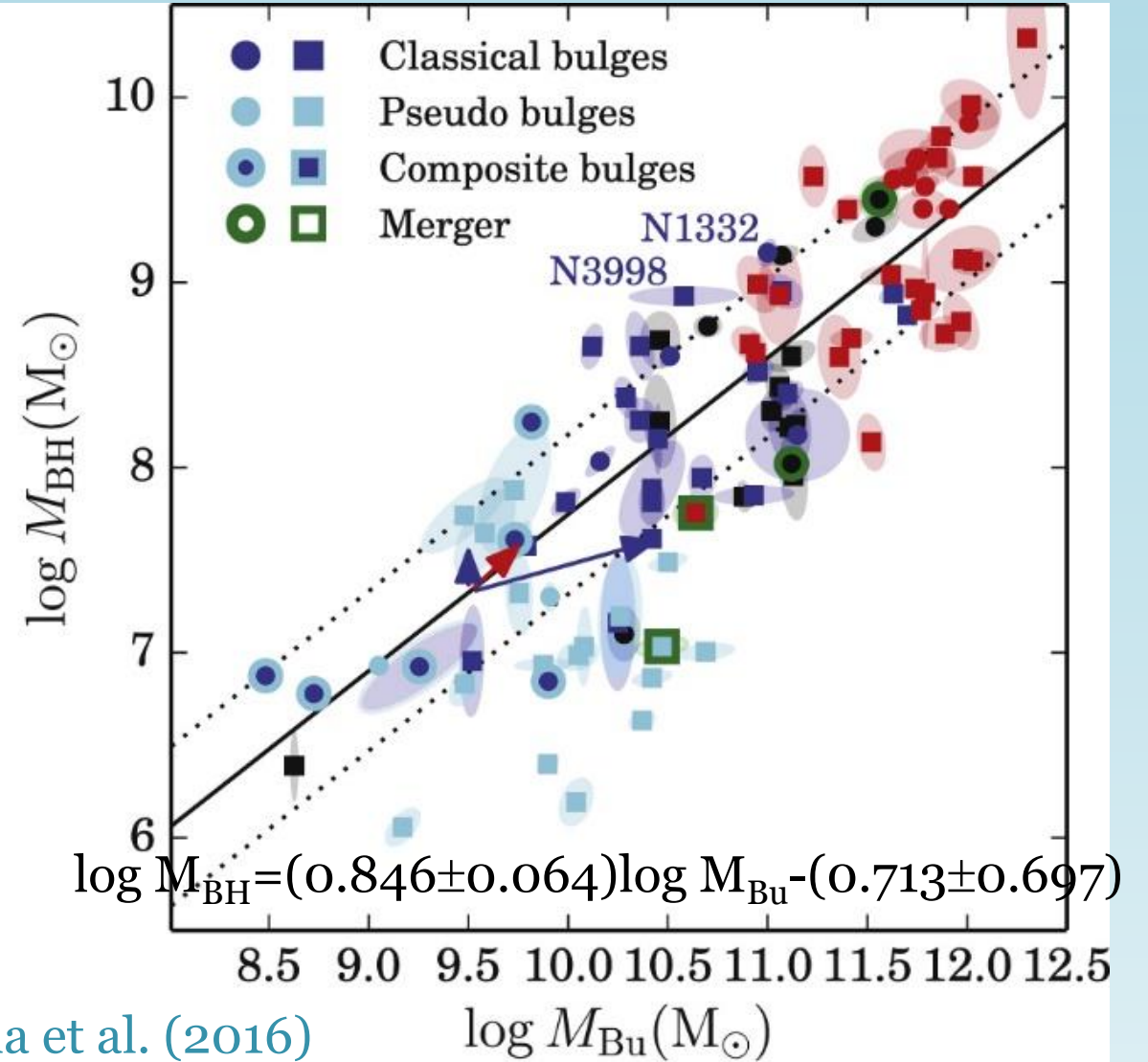
Star-formation timescale for massive ETGs

We have seen arguments showing that the star-formation timescale of massive ETGs is not determined by either the dynamical time, that would imply a longer SF timescale for the more massive galaxies, or by the merger timescale which is too short (and the merging sequence proceeds for too long).

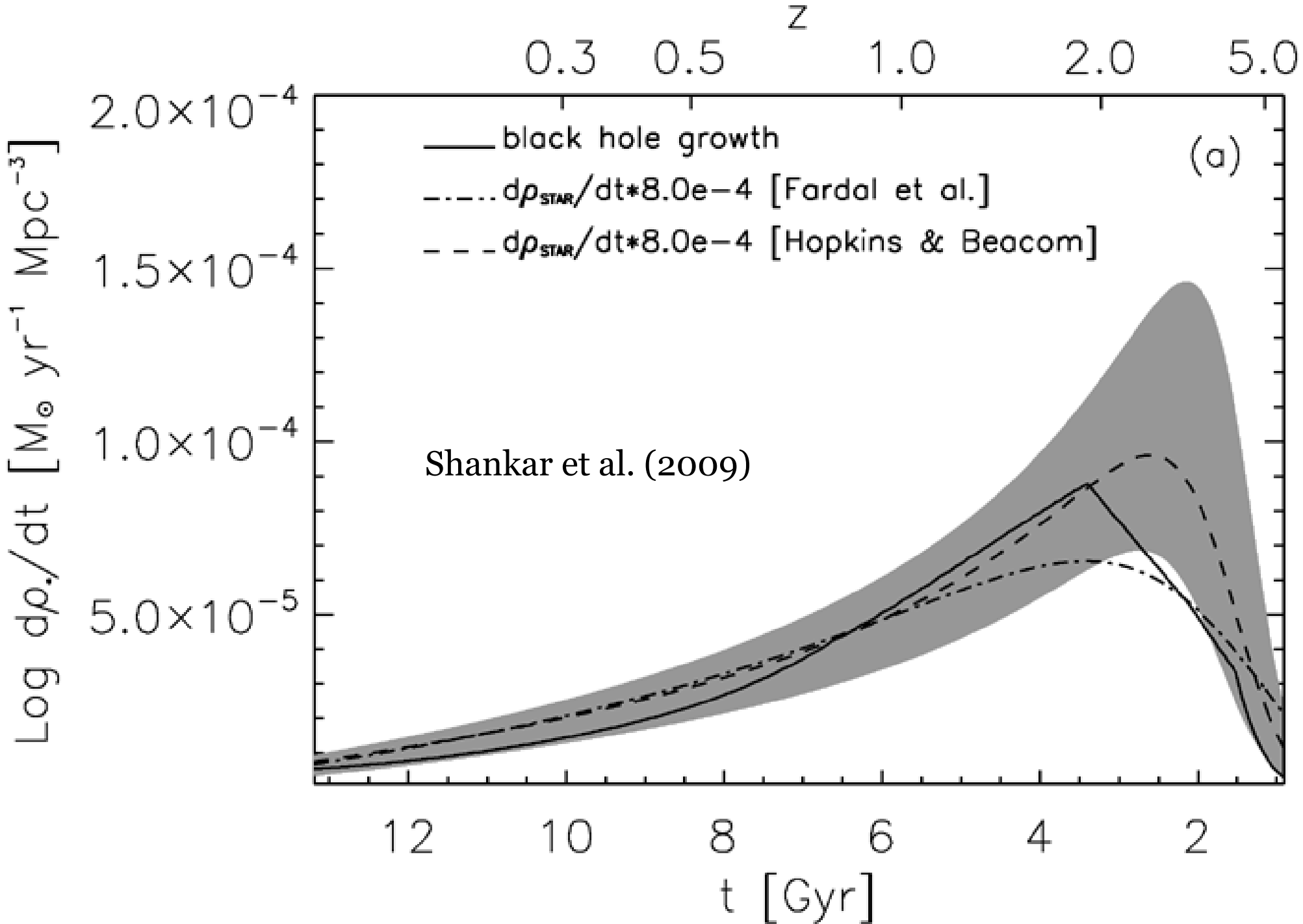
- SF on a dynamical (merger) timescale conflicts with the observed downsizing, with the colour-magnitude relation (massive ETGs would be too blue), with the colour- σ relation, with the line strength diagnostics of stellar populations (Lick indices), with the α -enhancement, with the uniformity of ETG properties demonstrated by the fundamental plane and hard to account for by a stochastic process such as a sequence of merger events, and with the abundance of bright sub-mm galaxies (SMGs),
- Which process then controls the SF timescale of massive ETGs? A plausible answer: AGN feedback.



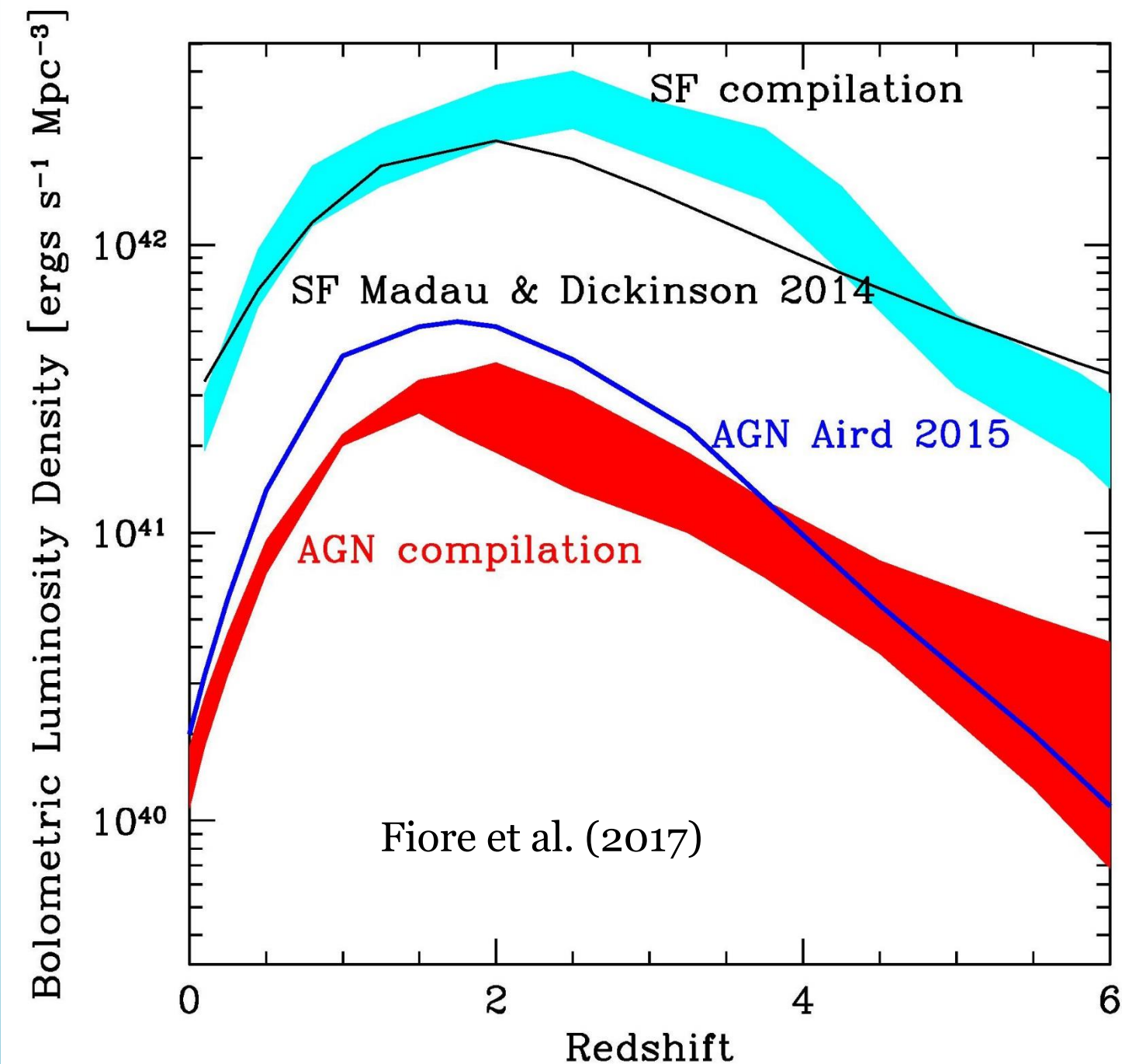
Saglia et al. (2016)



The ellipses show the 1σ errors. The labels name particularly deviant galaxies. The solid lines indicate the best-fit relations the ellipticals and classical bulges. The dotted lines indicate the estimated intrinsic scatter. Arrows describe the effect of an equal-mass dry merger (red), of a sequence of minor mergers doubling the bulge mass (orange), an equal-mass, gas-rich merger of two spiral galaxies with 20% bulge mass with bulge-scales ratio 3 (blue) or 0.5 (dashed blue), and doubling the BH mass through accretion or BH merging (black).

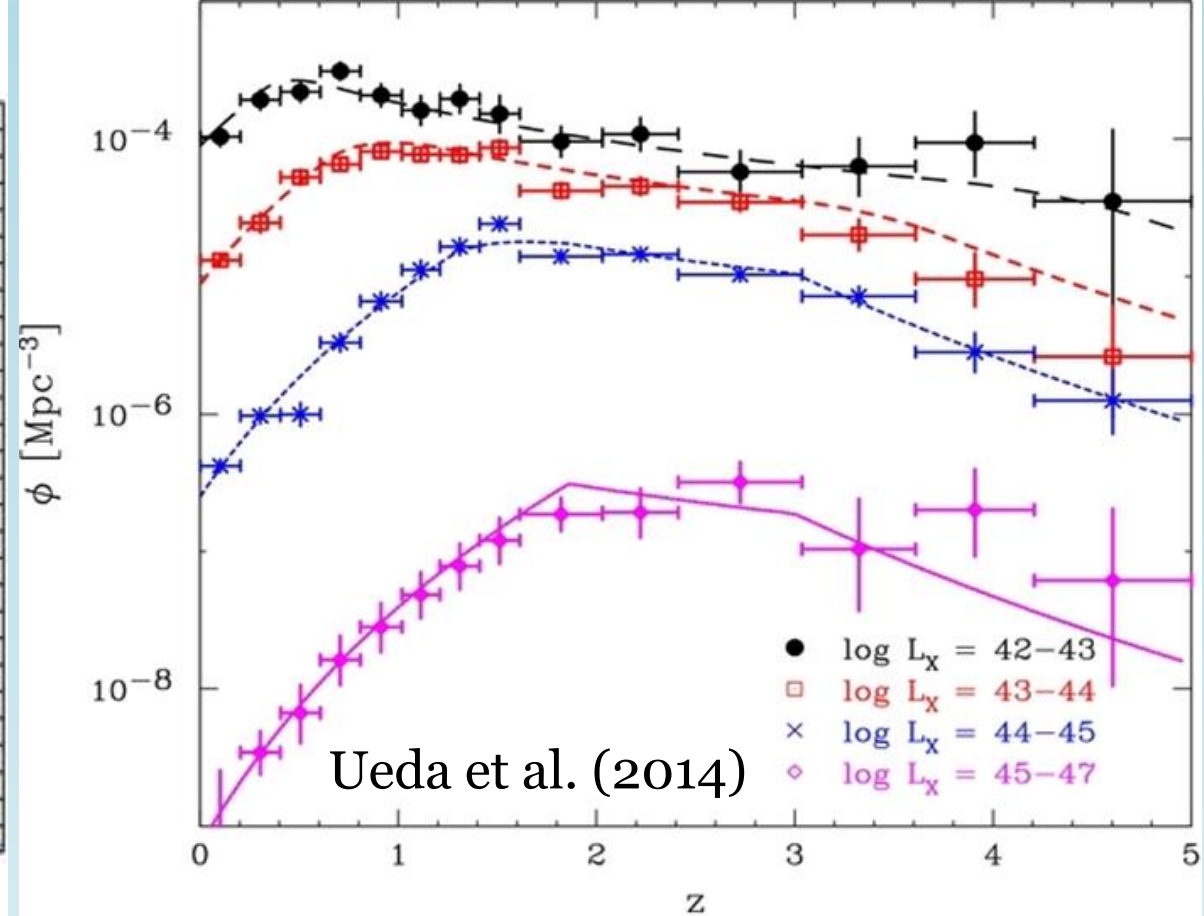
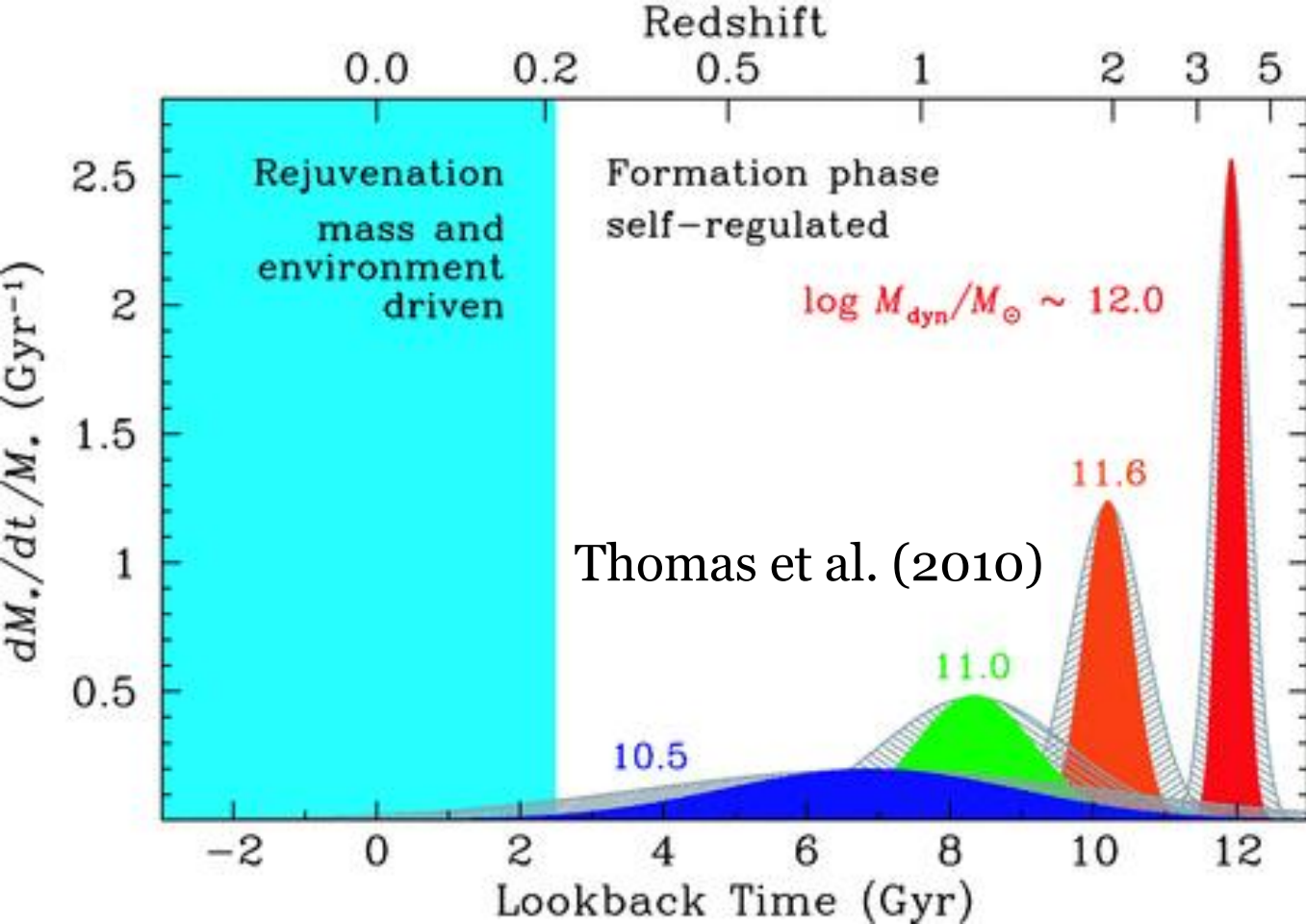


Average black hole accretion rate (solid line) compared to the SFR as given by Hopkins & Beacom (2006; dashed line) and Fardal et al. (2007; dot-dashed line), scaled by the factor $M_{\text{BH}}/M_{\text{STAR}} = 0.8 \times 10^{-3}$. The gray area shows the 3σ uncertainty region.



Evolution of the AGN bolometric luminosity density compared with the evolution of the luminosity density due to star formation. The red band has been computed from a compilation of X-ray luminosity functions and assuming the Marconi et al. (2004) bolometric correction. The blue solid line is the Aird et al. (2015) determination.

The cyan band is the average luminosity density due to star formation based on a compilation from Santini et al. (2009), Gruppioni et al. (2015), Bouwens et al. (2011, 2015). The black solid line is the Madau & Dickinson (2014) determination.



The growth histories of the stellar mass (left panel) and of the AGN luminosity (hence of BH mass) share further similarities: the most massive galaxies form in intense starbursts at high redshift while less massive galaxies have more extended star formation histories that peak later with decreasing mass. This ‘anti-hierarchical’ nature (*downsizing*) is mirrored in BH growth: the most massive BHs likely grow in intense quasar phases which peak in the early universe, while less massive BH have more extended, less intense growth histories that peak at lower redshift.

How can AGNs affect the host galaxy?

The BH's gravity has a negligible effect on its host galaxy. On the other hand, the energy released by the AGN

$$E_{\text{BH}} \simeq \epsilon M c^2 \sim 2 \times 10^{61} \frac{\epsilon}{0.1} \frac{M_{\text{BH}}}{10^8 M_{\odot}} \text{ erg},$$

where ϵ is the mass to radiation conversion efficiency, is far larger than the gas binding energy. Setting $M_{\text{gas}} = f M_{\text{bulge}}$, with $f < 1$, we have

$$E_{\text{gas}} \sim \frac{3}{2} f M_{\text{bulge}} \sigma^2 \sim 1.2 \times 10^{58} f \frac{M_{\text{bulge}}/M_{\text{BH}}}{10^3} \frac{M_{\text{BH}}}{10^8 M_{\odot}} \left(\frac{\sigma}{200 \text{ km/s}} \right)^{-2} \text{ erg},$$

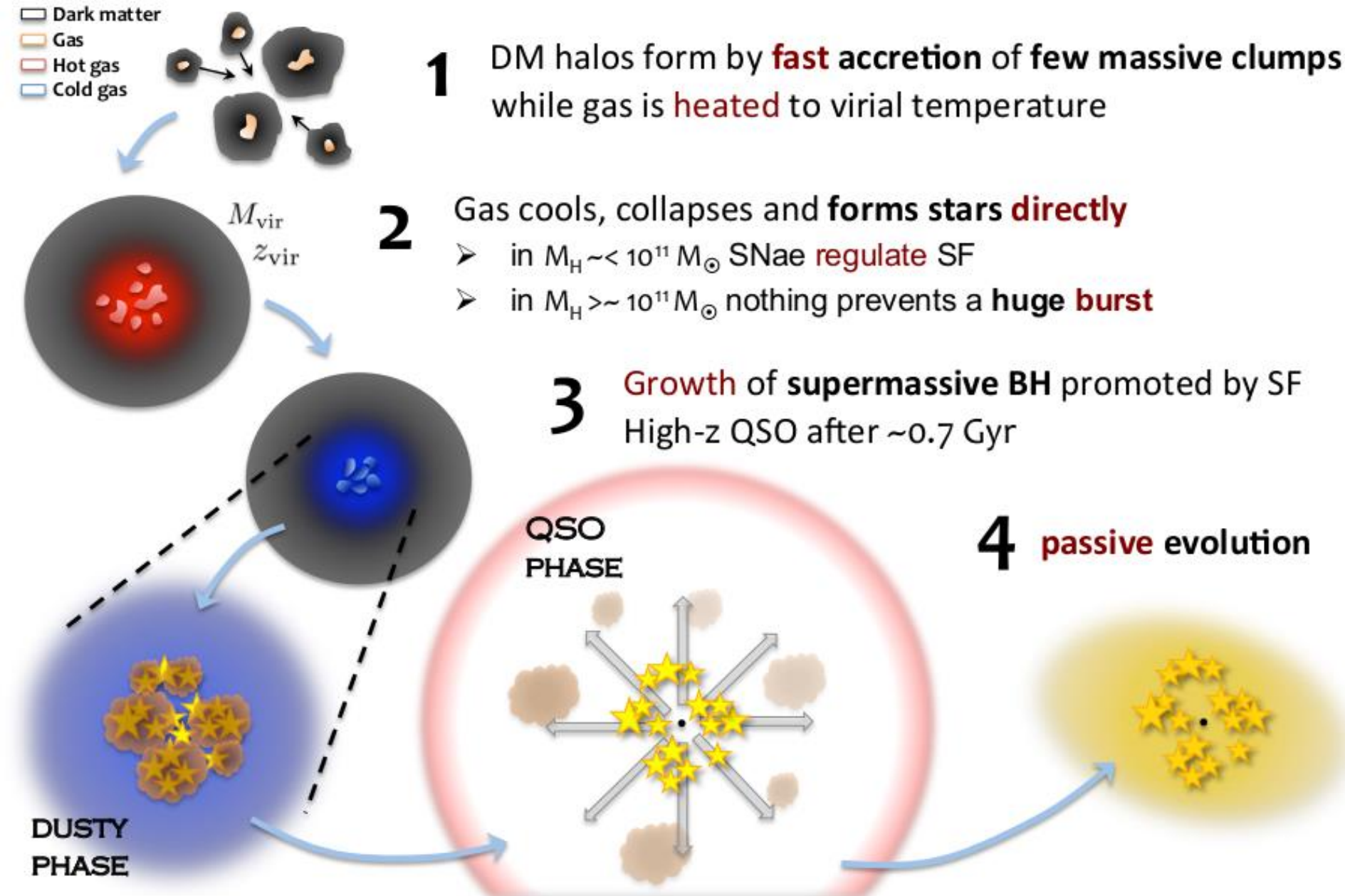
where σ is the line-of-sight velocity dispersion (the corresponding 3D velocity is $v = \sqrt{3}\sigma$). This means that only a few percent of the BH energy output may have a strong influence on the gas in the host galaxy, potentially expelling it and, at the same time, limiting its own growth.

AGN feedback

- ▶ Strong AGN-powered winds offer a plausible physical origin for the connections between the black hole and properties of its host and can determine the star formation timescale.
- ▶ The physical mechanism responsible for the AGN feedback is however still debated (see King & Pounds 2015 for an excellent review).
- ▶ To account for the observed downsizing either the fraction of AGN energy released in a mechanical form or the coupling with the gas must be somewhat higher for the more massive galaxies (Granato et al. 2004).

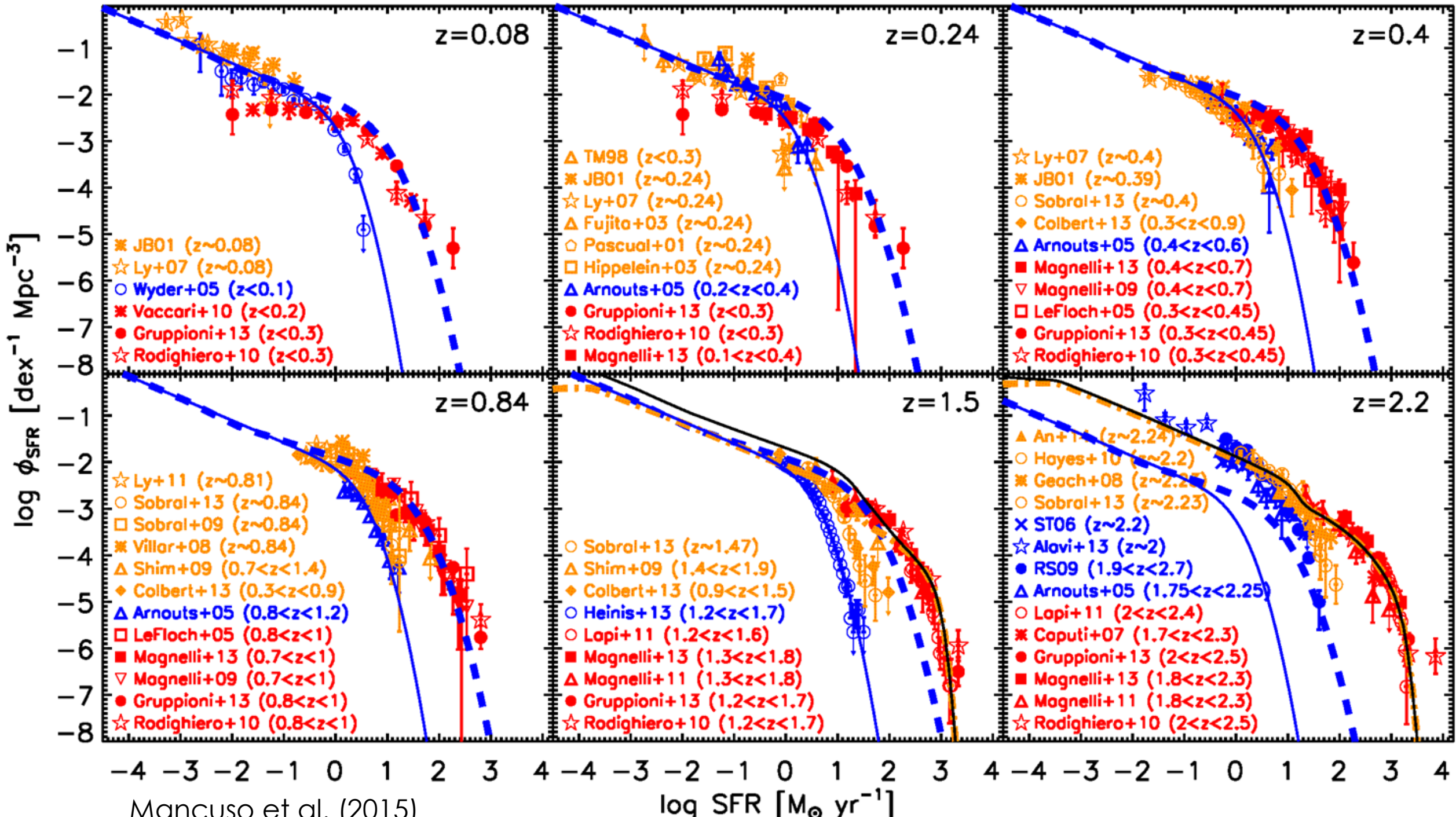
Self-regulated galaxy-AGN co-evolution

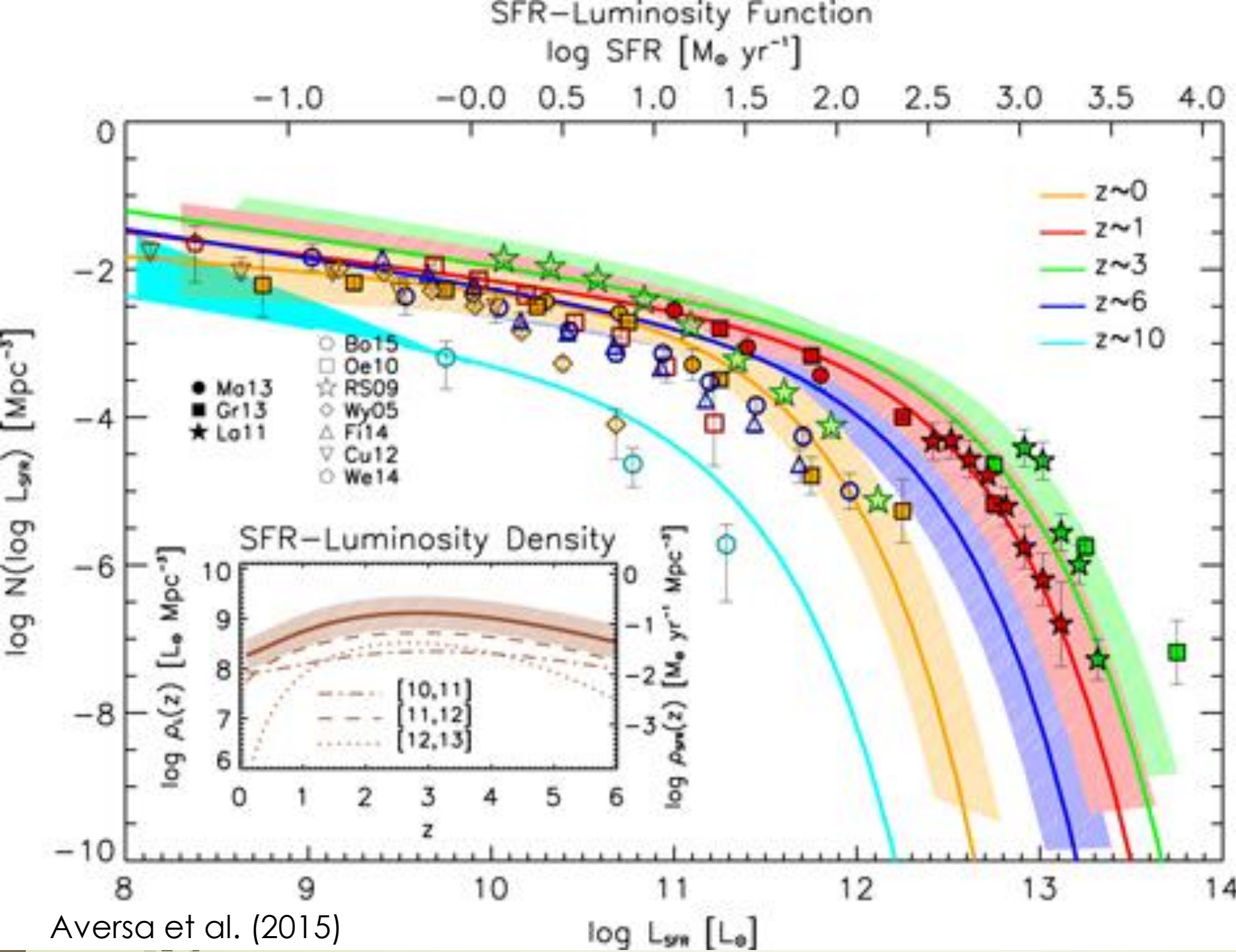
Based on the Granato et al. (2004) model. Figure: courtesy of M. Negrello.



Observed cosmic star formation history - 1

- There are many SFR indicators (see reviews by Kennicutt (1998) and Kennicutt & Evans (2012)). Such indicators generally measure the rate of massive star formation, because massive stars emit most of the energy from a young stellar population.
- Different observational tracers are sensitive to different ranges of stellar masses; hence, they respond differently as a function of stellar population age.
- H α emission arises primarily from HII regions photoionized by O stars with lifetimes shorter than 20 Myr, whereas the UV continuum is produced by stars with a broader mass range and with longer lifetimes.
- Optical/UV tracers of the SFR are liable to dust extinction that can be large, especially at high z , when the dusty ISM is abundant.
- Dust absorbs the starlight and reradiates it at MIR and FIR wavelengths. The effect of dust extinction at FIR wavelengths is generally regarded as negligible, although in the MIR extinction can still be relevant for the most deeply buried star formation and AGN.



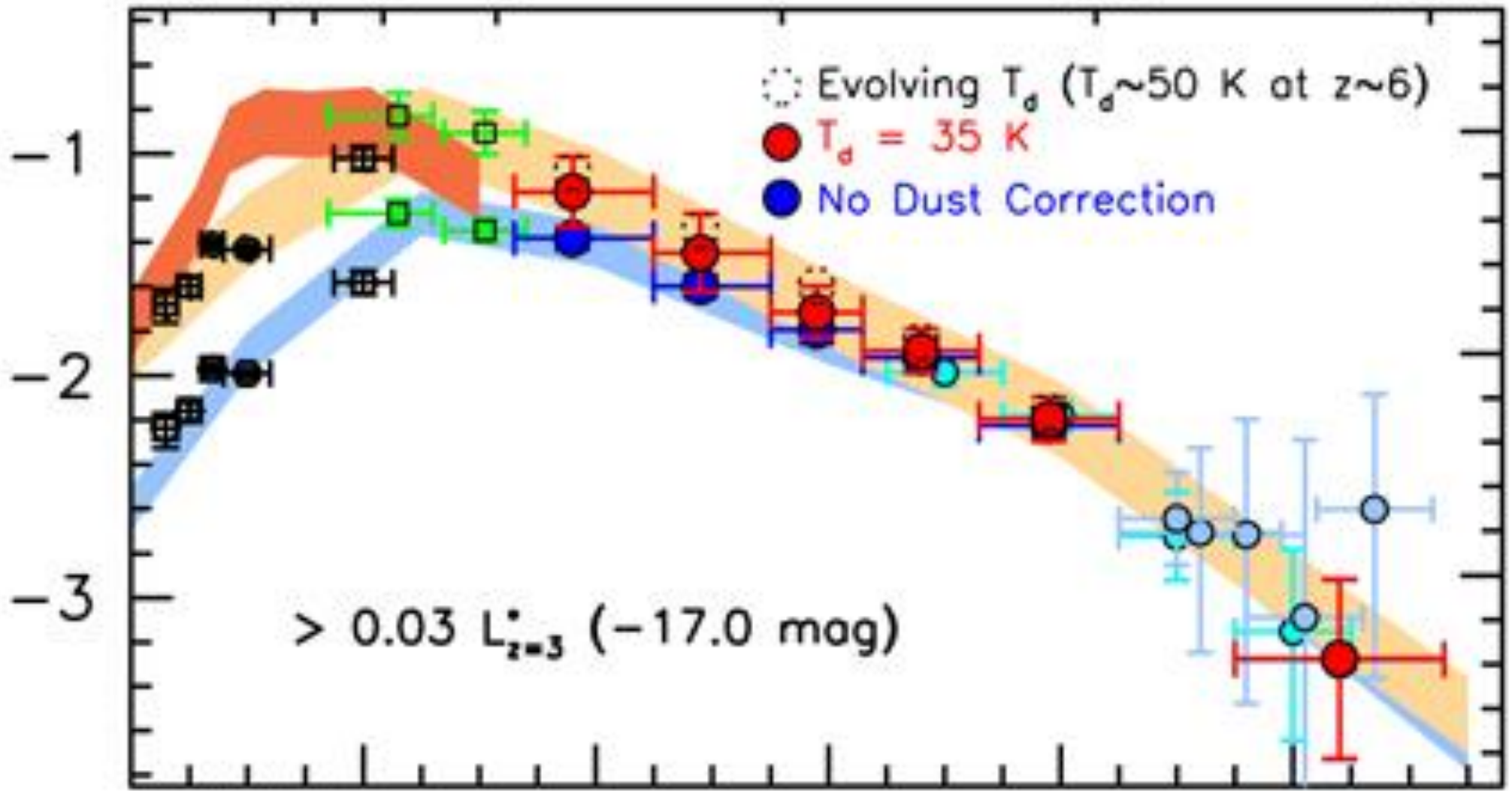


Bolometric luminosity function due to star formation as a function of the SFR at different redshifts. The solid lines show analytic fits of the luminosity functions and the hatched areas represent the uncertainty. The inset shows the SFR-luminosity density as a function of z , for the total luminosity range (solid line with hatched area), and for 3 ranges of $\log(L_{\text{SFR}}/L_{\odot})$. The maximum contribution comes from the range [11-12].

$\log \rho_{\text{SFR}} (M_{\odot} \text{ yr}^{-1} \text{ Mpc}^{-3})$

t (Gyr)

10 54 3 2 1 0.6 0.4



Bouwens et al. (2016)

z

Conclusions - 1

- The galaxy formation is quite inefficient: only about 10% of baryons are in galaxies. This calls for processes capable of hindering star formation and of cutting down exponentially the galaxy stellar mass function (feedback processes).
- The ratio of the stellar to halo mass function shows a well defined peak at $M_{\text{halo}} \sim 10^{12} M_{\text{SUN}}$, corresponding to $M_* \sim \text{few} \times 10^{10} M_{\text{SUN}}$, close to the boundary between the disk and the spheroid dominated stellar mass function.
- This mass also corresponds to $t_{\text{cool}} = t_{\text{dyn}}$ which is related to the disk/spheroid dichotomy (Eggen et al. 1962).
- Below this critical mass, the feedback from SNe dominates. For small halos a single SN can disrupt a proto-galaxy. For larger galaxies, the feedback involves the combined action of many SNe and the balance of the energy supplied by them with that dissipated in collisions between cold gas clouds. SN feedback can account for a typical star formation efficiency of 0.02.

Conclusions - 2

- Above that critical mass the AGN feedback provides a plausible explanation for the observed relationships between the black hole mass and properties of its host.
- The AGN feedback can also determine the star formation timescale for spheroidal galaxies and account for the observed “downsizing”.
- The narrowness of several well established relations (fundamental plane, the colour-magnitude, colour- σ) indicate that the properties of ETGs are remarkably uniform and that their star-formation history is primarily determined by the halo mass. This implies that stochastic events such as merger-driven starbursts play a relatively minor role.
- This conclusion is further supported by the abundance of bright submillimeter galaxies and by their clustering properties.

Conclusions - 3

- ▶ The global SFR density peaks at $z \sim 2.5$ i.e. ~ 3.5 Gyr after the Big Bang and drops exponentially at $z < 1$ with an e-folding timescale of 3.9 Gyr. The Universe was much more active place in the past: stars formed at a peak rate approximately almost one order of magnitude higher than is seen today.
- ▶ Approximately 25% of the present-day stellar mass density formed at $z > 2$, before the peak of the SFRD, and another 25% formed since $z = 0.7$, i.e., roughly over the last half of the Universe's age.
- ▶ The smooth evolution of the cosmic star formation history suggests that it is primarily determined by a balance between gas accretion and feedback processes, both closely related to galaxy mass. Again stochastic events such as merger-driven starbursts appear to have played a relatively minor role.